Università degli Studi di Padova
Dipartimento di Ingegneria dell'Informazione

Corso di Laurea Magistrale in Ingegneria delle Telecomunicazioni

Tesi di laurea magistrale

Analisi di protocolli HARQ per il sistema cellulare LTE

Analysis of HARQ protocols
for LTE cellular system

Candidato:
Marco Centenaro
Matricola 1043634

Relatore:
Chiar.mo Prof. Lorenzo Vangelista

Anno Accademico 2013–2014

Marco Centenaro: *Analysis of HARQ protocols for LTE cellular system,* Tesi di laurea magistrale, © luglio 2014.

Author's note.
This document was typeset using the LaTeX typographical style `classicthesis` developed by André Miede. This style was inspired by Robert Bringhurst's seminal book on typography *The Elements of Typographic Style* [1992]. `classicthesis` is available on CTAN (`http://www.ctan.org`).

Made on a Mac.

Final Version as of July 7, 2014 (`classicthesis`).

Non quia difficilia sunt non audemus, sed quia non audemus difficilia sunt.

— Lucius Annaeus Seneca

Coloro che s'innamorano di pratica senza scienza sono come nocchiero che entra in nave senza timone o bussola, che mai ha certezza dove va.

— Leonardo da Vinci

CONTENTS

LIST OF FIGURES

LIST OF TABLES

LIST OF ACRONYMS

ACMI	ACcumulated Mutual Information
ARQ	Automatic Repeat reQuest
AWGN	Additive White Gaussian Noise
CC	Chase Combining
CC-HARQ	Chase Combining Hybrid Automatic Repeat reQuest
CQI	Channel Quality Indicator
DCI	Downlink Control Information
DFT	Discrete Fourier Transform
eNB	Evolved NodeB
EPC	Evolved Packet Core
EPS	Evolved Packet System
e-UTRAN	Evolved Universal Terrestrial Radio Access Network
FDD	Frequency Division Duplex
FEC	Forward Error Correction
GSM	Global System for Mobile communications
HARQ	Hybrid Automatic Repeat reQuest
IP	Internet Protocol
IR	Incremental Redundancy
IR-HARQ	Incremental Redundancy Hybrid Automatic Repeat reQuest
OFDM	Orthogonal Frequency Division Multiplexing
OFDMA	Orthogonal Frequency Division Multiple Access
Layer 1	Physical Layer
LL	Link Layer
LTE	Long Term Evolution
MAC	Medium Access Control
MCS	Modulation and Coding Scheme
MIMO	Multi-Input Multi-Output
MRC	Maximum Ratio Combining

NAS	Non-Access Stratum
OFDM	Orthogonal Frequency Division Multiplexing
PAPR	Peak-to-Average Power Ratio
PDCP	Packet Data Convergence Protocol
PDU	Protocol Data Unit
QoS	Quality of Service
QPP	Quadratic Permutation Polynomial
RB	Resource Block
RE	Resource Element
RLC	Radio Link Control
RRC	Radio Resource Control
RV	Redundancy Version
SC-FDMA	Single-Carrier Frequency Division Multiple Access
SDU	Service Data Unit
SNR	Signal to Noise Ratio
SINR	Signal to Interference plus Noise Ratio
SISO	Single-Input Single-Output
SW	Stop-and-wait
SW-ARQ	Stop and Wait Automatic Repeat reQuest
TB	Transport Block
TDD	Time Division Duplex
TM	Transmission Mode
TTI	Transmission Time Interval
UCI	Uplink Control Information
UE	User Equipment
UMTS	Universal Mobile Telecommunications System

SOMMARIO

In questa tesi vengono studiati i protocolli di Hybrid-Automatic Repeat reQuest (HARQ) implementati nel sistema cellulare Long Term Evolution (LTE). Vengono ricavati modelli analitici dei suddetti protocolli e viene proposta una modifica che, utilizzando un approccio di tipo Bayesiano, ne migliora le prestazioni sia in termini di throughput che di ritardo. La quantificazione dei miglioramenti viene effettuata valutando i modelli proposti per via numerica. Il lavoro è stato ispirato dai requisiti delle reti cellulari 5G che sono in fase di definizione.

ABSTRACT

The aim of this thesis is studying the Hybrid-Automatic Repeat reQuest (HARQ) protocols that are implemented in the Long Term Evolution (LTE) cellular system. Analytical models of these processes are derived and an enhancement is proposed in order to increase the throughput and decrease the delivery delay, exploiting a Bayesian approach. A numerical evaluation of the performances has been carried out. The requirements for 5G networks are the main motivation for this work.

La forza di volontà attraversa anche le rocce.

— Proverbio giapponese

RINGRAZIAMENTI

Questo traguardo non sarebbe mai stato raggiungibile se non avessi avuto al mio fianco a sostenermi delle persone veramente speciali. Ringrazio, perciò, con tanto affetto i miei genitori, il mio grande fratello Stefano, nonni e zii, per tutto quello che hanno fatto per me. Inoltre un grande ringraziamento va ai miei amici e a Marika, per aver condiviso con me momenti indimenticabili.

Grazie a tutti, di cuore.

Padova, luglio 2014 M. C.

STRUTTURA DELLA TESI

Il presente elaborato è strutturato in 4 capitoli.

IL PRIMO CAPITOLO offre una breve introduzione sulla tecnologia del Long Term Evolution (LTE) e un primo accenno su come applicare un approccio bayesiano nel processo di trasmissione a livello link layer (LL).

IL SECONDO CAPITOLO fornisce una panoramica sullo stato dell'arte relativo allo studio di processi di Hybrid Automatic Repeat reQuest (HARQ).

IL TERZO CAPITOLO descrive come elaborare un modello del processo di HARQ e come sfruttarlo per valutare l'incremento delle prestazioni applicando l'approccio bayesiano.

IL QUARTO CAPITOLO contiene i risultati numerici e i grafici relativi alle prestazioni del sistema.

1 INTRODUCTION

1.1 A BRIEF INTRODUCTION TO LTE

Long Term Evolution (LTE) is a standard for cellular wireless communication of high-speed data for mobile phones and data terminals. It is based on the Global System for Mobile communications (GSM) and Universal Mobile Telecommunications System (UMTS) network technologies, increasing capacity and speed using a different radio interface together with core network improvements. As its predecessors, this standard is developed by the 3GPP association (3rd Generation Partnership Project)[1].

LTE or the Evolved Universal Terrestrial Radio Access Network (e-UTRAN) is the access part of the Evolved Packet System (EPS), which is purely Internet Protocol (IP) based. This new access solution is based on Orthogonal Frequency Division Multiple Access (OFDMA). In combination with higher order modulation (up to 64-QAM), large bandwidths (up to 20 MHz) and *spatial multiplexing* in the downlink (up to 4×4-MIMO) high data rates can be achieved. The highest theoretical peak data rate on the transport channel is 75 Mbps in the uplink and up to 300 Mbps in the downlink.

To enable possible deployment around the world, supporting as many regulatory requirements as possible, LTE is developed for a number of frequency bands currently ranging from 700 MHz up to 2.7 GHz. The available bandwidths are also flexible, starting with 1.4 MHz up to 20 MHz.

1.2 NETWORK ARCHITECTURE

The network architecture of LTE (also known as EPS) consists of three main components:

- the User Equipment (UE). The internal architecture of the UE for LTE is identical to the one used by UMTS and GSM which is actually a Mobile Equipment.
- the e-UTRAN (access network). The e-UTRAN handles the radio communications between the mobile and the core network and has just one component: the Evolved NodeB (eNB). Each eNB is a base station that controls the mobiles in one or more cells; the base station that is communicating with a mobile is known as its serving eNB. Each eNB connects with the EPC by means of the S1 interface and it can also be connected to nearby base stations by the X2 interface to perform signaling and packet forwarding during handover.
- the Evolved Packet Core (EPC). It represents the core network of the system, performing switching, authentication and connection to other packet (IP) networks and telephone networks.

A graphical representation of the LTE network architecture is shown in Figure 1.

1 http://www.3gpp.org, last visited July 7, 2014

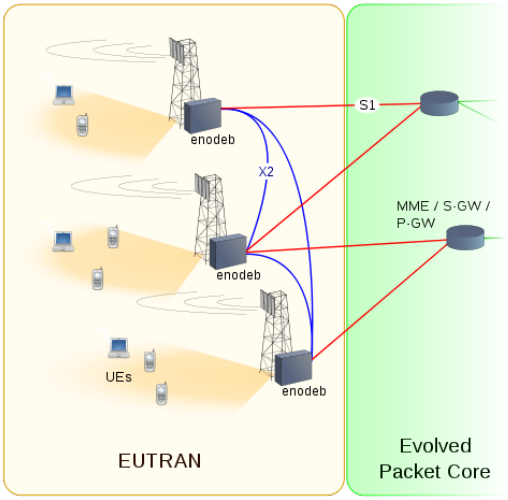

Figure 1: LTE network architecture.

1.3 PROTOCOL STACK

The LTE protocol stack is organized as follows:

- the Physical Layer (Layer 1) carries all information from the MAC transport channels (see 1.4) over the air interface.
- the Medium Access Control (MAC) is responsible for mapping between logical channels and transport channels (see 1.4), multiplexing/demultiplexing MAC Service Data Units (SDUs) from logical channels into Transport Blocks (TBs) to be delivered to/delivered by the Layer 1 on transport channels, error correction through HARQ (see 1.8).
- the Radio Link Control (RLC) is responsible for transfer of upper layer Protocol Data Units (PDUs), error correction through Automatic Repeat reQuest (ARQ), concatenation, segmentation and reassembly of RLC SDUs.
- the Radio Resource Control (RRC) provides services such as broadcast of system information, paging, establishment, maintenance and release of an RRC connection between the UE and e-UTRAN, security.
- the Packet Data Convergence Protocol (PDCP) is responsible for header compression/decompression of IP data, in-sequence delivery of upper layer PDUs, duplicate discarding.
- the Non-Access Stratum (NAS) supports the mobility of the UE and the session management procedures to establish and maintain IP connectivity.

A graphical representation of it is shown in Figure 2.

1.4 TYPES OF CHANNELS

In LTE three categories of channels are defined:

LOGICAL CHANNELS These channels define *what type* of information is transmitted over the wireless channel, either data or control messages. The MAC provides services to the RLC in the form of logical channels.

TRANSPORT CHANNELS They define *how* and *with what characteristics* the information is transmitted over the radio interface. The MAC layer uses services from the Layer 1 in the form of transport channels.

PHYSICAL CHANNELS They correspond to sets of time-frequency resources (see 1.7) used for transmission of a particular transport channel. Each transport channel is mapped to a corresponding physical channel, but there are also physical channels without a corresponding transport channel: these channels are used for Downlink Control Information (DCI), providing the terminal with the necessary information for proper reception and decoding of the downlink data transmission, and Uplink Control Information (UCI) used for providing the scheduler and the Hybrid Automatic Repeat reQuest (HARQ) protocol with information about the situation at the terminal.

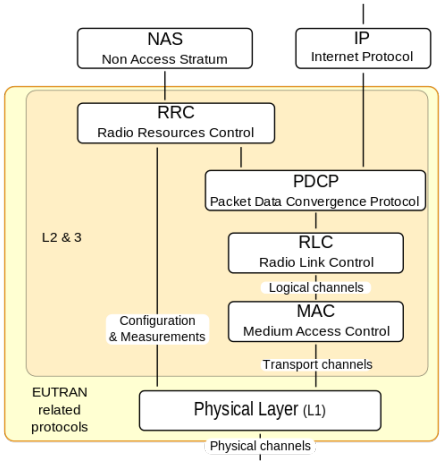

Figure 2: LTE protocol stack.

1.5 OFDM, OFDMA AND SC-FDMA

To overcome the effect of multipath fading, LTE uses Orthogonal Frequency Division Multiplexing (OFDM) for the downlink, exploiting a large number of narrow subcarriers for multi-carrier transmission to carry data instead of spreading one signal over the entire bandwidth. In OFDMA these subcarriers can be shared between multiple users. The OFDMA solution leads to high Peak-to-Average Power Ratios (PAPRs), requiring expensive power amplifiers with hard requirements on linearity and, therefore, increasing the power consumption for the transmitter. This is not a problem if the transmitter is the eNB, i.e, in the downlink, but it becomes a problem if the transmitter is the UE. Hence a different solution has been designed for the uplink: the Single-Carrier Frequency Division Multiple Access (SC-FDMA) solution generates a signal with single carrier characteristics, i.e., with a low PAPR, by grouping together the resource blocks (see 1.7).

1.6 DUPLEX SCHEMES

LTE is developed to support both the Frequency Division Duplex (FDD) and the Time Division Duplex (TDD). In FDD uplink and downlink transmissions use disjoint frequency bands, whereas in TDD they share the same carrier but are separated in time. In TDD and FDD up to 15 and 8 HARQ process are considered in parallel, respectively.

1.7 TIME–FREQUENCY RESOURCES AND SCHEDULING

LTE considers a slotted time axis in which:

- one *frame* lasts $T_{\text{frame}} = 10$ ms;
- each frame is composed of 10 *subframes* of duration $T_{\text{subframe}} = 1$ ms;
- every subframe is divided into 2 *time slots* of duration $T_{\text{slot}} = 0.5$ ms;
- every slot contains 7 OFDM symbols: $T_{\text{symbol}} = 0.067$ ms[2].
- every OFDM symbol contains up to 2048 OFDM samples: $T_s = 0.325$ ns.

Considering T_s as the basic time unit, we can express the other quantities in function of it as:

$$\begin{aligned} T_{\text{symbol}} &= 2048 \cdot T_s \\ T_{\text{slot}} &= 15360 \cdot T_s \\ T_{\text{subframe}} &= 30720 \cdot T_s \\ T_{\text{frame}} &= 307200 \cdot T_s \end{aligned}$$

The subframe duration is also denoted as Transmission Time Interval (TTI):

$$T_{\text{subframe}} = \text{TTI}$$

For what concerns the frequency bands, instead, many possibilities in terms of carrier frequency f_c and bandwidth $\mathcal{B}$ are available. In every case, the total band is split into sub-bands of 180 kHz bandwidth, each one containing 12 subcarriers spaced of 15 kHz. We call Resource Block (RB) the time-frequency unit of 0.5 ms times 180 kHz and Resource Element (RE) the time-frequency unit of one OFDM symbol times one subcarrier. Thus, each RB consists of $7 \cdot 12 = 84$ REs. In LTE the time-frequency resources are shared between users and they are dynamically assigned by the scheduler in terms of *resource-block pairs*, i.e., couples of RB (time-frequency units of 1 ms times 180 kHz).

Figure 3 may explain better the structure of the time axis; Figure 4, instead, shows the time-frequency grid structure in LTE.

2 $T_{\text{symbol}} < T_{\text{slot}}/7$ because we must account for the cyclic prefix.

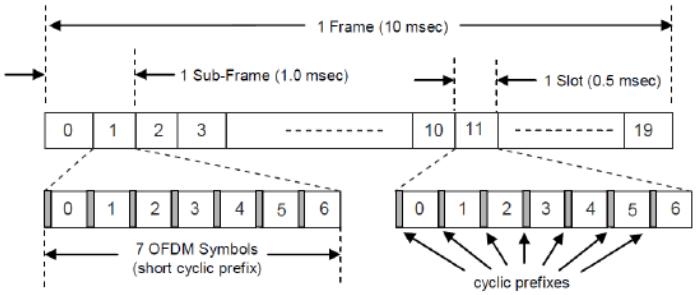

Figure 3: LTE frame structure.

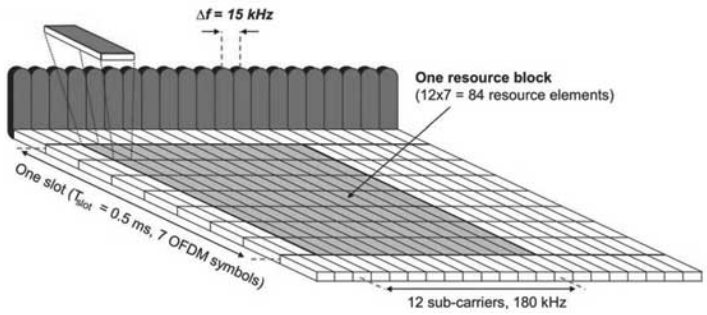

Figure 4: LTE time-frequency structure.

1.8 THE LTE MAC LAYER

All Layer 1 transport data are encoded using a turbo code with a Quadratic Permutation Polynomial (QPP) internal interleaver. We recall that a permutation polynomial, for a given ring, is a polynomial that acts as a permutation of the elements of the ring; it is quadratic if the polynomial is of degree two. Since the receiver is capable of asking for a retransmission of the packet in case of decoding failures, an ARQ retransmission process is employed on top of the Forward Error Correction (FEC) turbo code, establishing an overall Hybrid Automatic Repeat reQuest (HARQ) process. The applied ARQ process is a Stop and Wait Automatic Repeat reQuest (SW-ARQ) one.

The coding rate of the mother turbo code is

$$R_c = \frac{1}{3}$$

however many other coding schemes are available thanks to puncturing patterns provided in the rate matching process after the encoding block. The patterns are selected according to the Channel Quality Indicator (CQI) index. The CQI is a parameter that indicates the *state* of the channel (whether it is *good* or *bad*), using a scale of 15 values; this piece of information is reported to the source by the destination, together with the acknowledgment/not-acknowledgement of the previously transmitted packet. The type of digital modulation is selected depending on the CQI value, so the modulation in LTE is adaptive.

1.9 DOWNLINK HARQ AND UPLINK HARQ

A HARQ process in LTE can be

- *synchronous*: the retransmissions take place after a constant period of time
- *asynchronous*: the retransmissions can take place whenever in time, due to scheduling purposes. In this cases we need an appropriate signaling to make the transmitter aware of which HARQ process we are considering.

We can distinguish also between other two kinds of HARQ process:

- *adaptive*: the transmission parameters (including the Redundancy Version, see 2.4.1) are decided on the fly by the scheduler
- *non-adaptive*: the transmission parameters are those that have been defined at the first transmission attempt and they don't change. In this case subsequent retransmissions take progressive Redundancy Version indexes.

Depending on the direction of the transmission, in LTE we have that

- the downlink HARQ is *asynchronous* and *adaptive*
- the uplink HARQ is *synchronous* and *non-adaptive*.

1.10 BEYOND LTE

Recent studies and extrapolations from past developments predict a total traffic increase by a factor of 500 to 1000 within the next decade. These figures assume approximately a 10 times increase in broadband mobile subscribers, and 50-100 times higher traffic per user. Besides the overall traffic, *the achievable throughput per user has to be increased significantly*. A rough estimation predicts a minimum 10 times increase in average, as well as in peak, data rate.

Moreover, essential design criteria, which have to be fulfilled more efficiently than in today's systems, are fairness between users over the whole coverage area, *latency to reduce response time* and better support for a multitude of Quality of Service (QoS) requirements originating from different services[3].

1.11 HOW TO APPLY INTELLIGENCE?

In the LTE uplink, which is synchronous and non-adaptive, the Modulation and Coding Scheme (MCS) is determined by the last CQI index that the source reads in the feedback packet sent by the destination. However, this approach may let us experience inefficiencies in some cases, e.g. in case of *deep fading* events, in which the transmitter employs the most resilient MCS for the next transmission attempt even though the channel becomes *good*

3 http://www.networks-etp.eu/fileadmin/user_upload/Home/draft-PPP-proposal.pdf, last visited July 7, 2014

again, yielding an inherent throughput reduction. On the opposite side, if we experience a very favourable (but instantaneous) condition for the channel then we may employ a too optimistic MCS, causing a sequence of failed transmissions and yielding again to a throughput reduction.

We would like to propose a *Bayesian approach*, in which the network

1. *observes* how the channel changes over time, storing data in a *cognitive repository*,
2. *learns* from the gathered data,
3. *plans* the action, trying to predict the future behaviour of the channel and finally
4. *acts*, tuning the MCS appropriately in order to increase the throughput of the system.

2 STATE OF THE ART

2.1 WHAT IS HARQ?

In Chapter 1 we mentioned that LTE MAC layer employs jointly a FEC turbo coding approach and a SW-ARQ retransmission process, i.e., a HARQ process. According to the literature, two kinds of HARQ processes are usually considered, depending on how the receiver treats the erroneously received packets:

HARQ-TYPE I After each transmission attempt the received packet is discarded if it is erroneous.

HARQ-TYPE II After each transmission attempt the received packet, if erroneous, is stored in a buffer and then *combined* with subsequent transmitted packets, in order to increase the performances of the FEC code. We can make a further distinction between the following two subcategories of HARQ-II processes, depending on *how* the receiver combines the multiple versions of the erroneously received packets:

CC-HARQ If the transmission involves always the same packet in different attempts then we have a Chase Combining Hybrid Automatic Repeat reQuest (CC-HARQ); at the receiver side a Maximum Ratio Combining (MRC) of the received replicas is applied in order to improve resiliance to noise and, therefore, the FEC performances.

IR-HARQ In Incremental Redundancy Hybrid Automatic Repeat reQuest (IR-HARQ), instead, the transmitter splits the entire coded message in sub-codewords that are sent in subsequent transmission attempts; the receiver combines them appropriately.

We will see in the next sections that LTE follows a mixed approach, using both CC-HARQ and IR-HARQ.

2.2 BLOCK SCHEME

In Figure 5 the block scheme of an LTE transmission, from channel coding till physical transmission over the wireless channel, is depicted. First of all there is the turbo encoding procedure, then the selection of the appropriate MCS according to the channel conditions, the antenna mapping and the OFDM modulator. In this thesis we will focus on the MCS selection block.

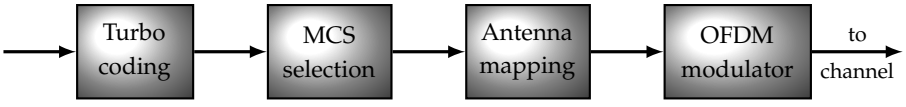

Figure 5: Block scheme of a packet transmission, from channel encoding procedure till the data transmission over the wireless channel.

2.3 TURBO CODING

The FEC part of the HARQ framework is performed by a turbo code of mother code rate

$$R_c = \frac{1}{3}$$

The encoding process consists of two rational, rate-1/2 constituent encoders with generating vector

$$\mathbf{g}(D) = \begin{bmatrix} 1 \\ \frac{1+D+D^3}{1+D^2+D^3} \end{bmatrix}$$

in combination with QPP interleaving, which provides a mapping from the input (non-interleaved) bits to the output (interleaved) bits according to the function

$$\Pi(i) = \left(f_1 i + f_2 i^2\right) \mod K$$

where

- i is the index of the input bit in the original sequence
- $\Pi(i)$ is the index of the same bit in the interleaved sequence
- K is the block length
- f_1 and f_2 are parameters that depend on the value of K.

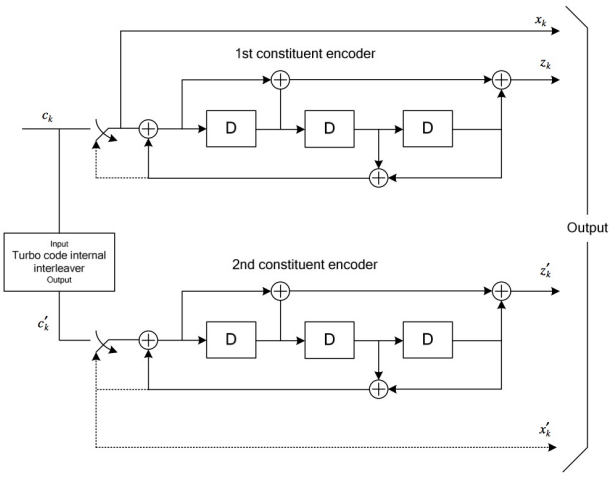

Figure 6: Block diagram of LTE Turbo encoder.

In Figure 6 the block diagram of LTE Turbo encoder is depicted. It can seen that the encoding procedure produces three bit streams:

1. the first stream contains the unprocessed input bits, i.e. the *systematic bits*
2. the second stream is the one that carries the parity bit produced by the first constituent encoder, i.e. the *first parity bits*
3. the third stream carries the parity bits generated by the second constituent encoder, i.e. the *second parity bits*.

Therefore, this turbo code is *systematic* since the input data is embedded in the first part of the encoded output sequence.

2.4 MODULATION AND RATE MATCHING

2.4.1 Circular buffer

The three output streams of the Turbo encoder experience a row-column interleaving separately and they are inserted in a *circular buffer* (see Figure 7) where the systematic bits fill the first positions, followed by alternating insertions of the first and second parity bits (*interlacing* procedure). A subset of consecutive bits called Redundancy Version (RV) is then extracted from the circular buffer; the size of this subset is such that it matches the number of avaliable resource elements in the resource blocks assigned for the transmission. The exact set of extracted bits depend on the RV index, corresponding to different starting points for the extraction of coded bits from the circular buffer. There are four alternatives for the RV, as many as the allowed transmission attempts. The selection of the appropriate subset of bits is done by the *bit selection* block.

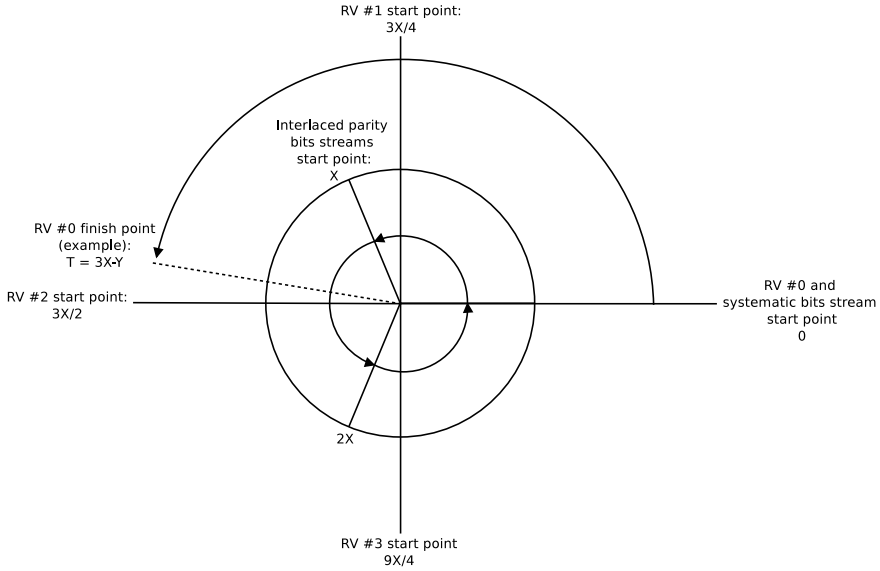

Figure 7: LTE circular buffer structure: we can distinguish the systematic bits block (from 0 to X = number of systematic bits) and the interlaced parity bits block (from X to 3X). Note also the four starting points for the extractions of the bits for the different RVs.

2.4.2 Bit selection

The puncturing patterns for the RV bit selection depend on the value of the CQI, which is the numerical index that indicates how good the channel is. In LTE there exist $N = 15$ values for the CQI (integer values belonging to the set $\{1, \ldots, 15\}$), each one corresponding to a particular MCS that is required for the next packet transmission. In literature [Kwan and Ikuno, 2013] we can find methods to analitically characterize the code rate we obtain after the n-th transmission attempt, using a combination of an inner channel code processing unrepeated bits with a code rate of $R_c^{(n)}$ and an outer repetition code with rate $1/N_n$ working on the output of the preceding channel code.

Theorem 1 (Effective code rate modelling in LTE)**.** *If the redundancy versions* 0–3 *are invoked sequentially then the code rate* $R_c^{(n)}$ *and level of repetition* N_n *associated with retransmission index* $n \in \{0,1,2,3\}$ *(*$n = 0$ *is the first transmission attempt) can be expressed as*

$$R_c^{(n)} = \max\left\{\frac{4}{3n+4(3-\eta)}, \frac{1}{3}\right\}$$

$$N_n = \max\left\{R_c^{(n)} \cdot n(3-\eta), 1\right\}$$

where η *is defined as the ratio between the number of puntured bits* Y *over the number of systematic bits* X*.*

Proof. Let T be the amount of bits taken from the circular buffer:

$$T = 3X - Y = X\left(3 - \frac{Y}{X}\right) = X(3-\eta)$$

Let the code rate $R_c^{(n)}$ be the ratio between the systematic bits and the total number of systematic and parity transmitted until transmission index n. Knowing that the starting position of the circular buffer can be easily characterized by

$$S_n = k_0 + n\left(\frac{3}{4}X\right)$$

where k_0 is the non-zero start position for the selection of the bits of the RV of index 0; without losing generality we can impose $k_0 = 0$. Now if we consider the transmission index $n = 0$ (first transmission attempt) it is trivial to see that

$$R_c^{(0)} = \max\left(\frac{X}{T}\,;\frac{1}{3}\right)$$

For the transmission index $n = 1$, instead, we have that

$$R_c^{(1)} = \max\left(\frac{X}{S_1 + T}\,;\frac{1}{3}\right)$$

and going on for the generic transmission index n we get

$$\begin{aligned} R_c^{(n)} &= \max\left(\frac{X}{S_n + T}\,;\frac{1}{3}\right) = \max\left(\frac{X}{\frac{3}{4}Xn + 3X - Y}\,;\frac{1}{3}\right) = \\ &= \max\left(\frac{4}{3n+4(3-\eta)}\,;\frac{1}{3}\right) \end{aligned}$$

For what concerns the redundancy due to repetition, it can be expressed as

$$N_n = \frac{R_c^{(n)}}{X/(nT)} = R_c^{(n)} \cdot n(3-\eta)$$

Note that N_n can be smaller than 1 if no bits are repeated but some bits are punctured: in this case, the total number of transmitted bits should be the same as the total number of coded bits. Therefore the final formula is

$$N_n = \max\left(R_c^{(n)} \cdot n(3-\eta)\,;1\right)$$

□

Please note that, as it is defined, $R_c^{(n)}$ is *not* the coding rate of the retransmission of index n, but the *effective* code rate *after* the n-th retransmission (without considering the repeated bits, i.e., considering the saturation of the rate to the mother code rate of $1/3$ in those cases in which $S_n + T$ exceeds the size of the circular buffer).

The modulation and coding schemes which are available in LTE are shown in Table 1. In the same Table the values of η for all the CQI indexes can be found; these values have been computed inverting the previous expression:

$$R_{c,REP}^{(0)} = \frac{4}{3 \cdot 0 + 4(3-\eta)} = \frac{1}{3-\eta} \Rightarrow \eta = 3 - \frac{1}{R_{c,REP}^{(0)}}$$

where the values of $R_{c,REP}^{(0)}$ can be found in Ikuno *et al.*, 2011. The available code rates for the different RVs are shown in Figure 8.

Table 1: Modulation and coding schemes in LTE. $R_c^{(0)}$ and $R_{c,REP}^{(0)}$ indicate the code rate of the first transmission attempt without considering the repeated bits and considering them, respectively.

CQI k	Modulation	η	$R_c^{(0)}$	$R_{c,REP}^{(0)}$
1	QPSK	−10.1300	1/3	0.076
2	QPSK	−5.5300	1/3	0.12
3	QPSK	−2.3100	1/3	0.19
4	QPSK	−0.3200	1/3	0.30
5	QPSK	0.7200	0.44	0.44
6	QPSK	1.3000	0.59	0.59
7	16-QAM	0.2900	0.37	0.37
8	16-QAM	0.9100	0.48	0.48
9	16-QAM	1.3400	0.60	0.60
10	64-QAM	0.8000	0.45	0.45
11	64-QAM	1.1900	0.55	0.55
12	64-QAM	1.4600	0.65	0.65
13	64-QAM	1.6700	0.75	0.75
14	64-QAM	1.8300	0.85	0.85
15	64-QAM	1.9200	0.93	0.93

2.4.3 Digital modulation

The block of bits delivered by the HARQ functionality is then multiplied (exclusive-OR operation) by a bit-level scrambling sequence and the mapping to complex modulation symbols is finally performed according to one of the following digital modulation schemes:

1. QPSK
2. 16-QAM
3. 64-QAM

corresponding to two, four or six bits per symbol, respectively.

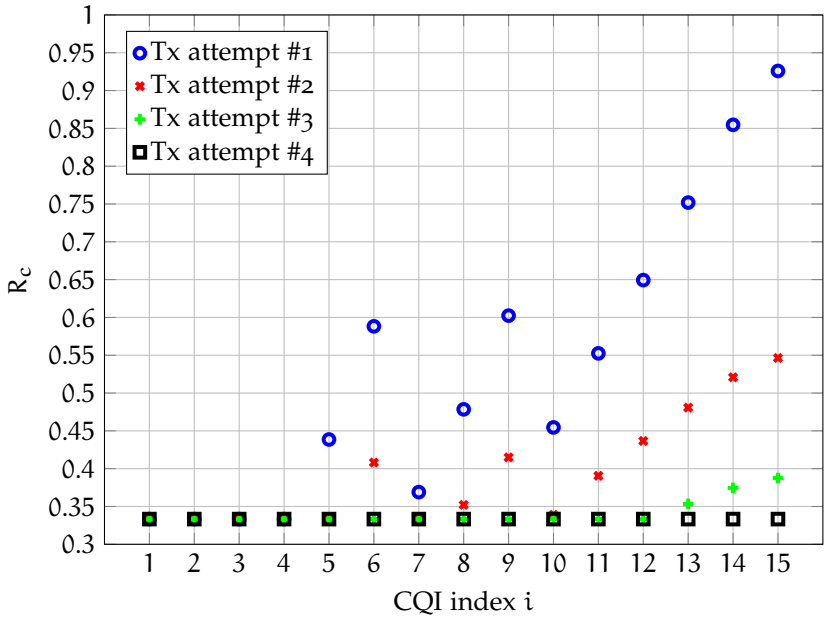

Figure 8: Code rates for subsequent transmission attempts. The rates are considered effective and without considering repeated bits.

2.5 ANTENNA MAPPING AND OFDM MODULATOR

The output of the data modulation is then mapped to different antenna ports. The input of the antenna mapping consists of the modulation symbols (QPSK, 16-QAM, 64-QAM) corresponding to one or two transport blocks. In fact, there is only one transport block per transmission time slot (TTI) except for spatial multiplexing, in which there may be two transport blocks per TTI. The output of the antenna mapping is a set of symbols for each antenna port, which are applied to the Orthogonal Frequency Division Multiplexing (OFDM) modulator, i.e., mapped to the basic OFDM time-frequency grid corresponding to that antenna port.

The different multi-antenna transmission schemes correspond to different Transmission Mode (TM). In LTE 9 different transmission modes are defined:

1. single-antenna transmission
2. transmit diversity
3. open-loop spatial multiplexing
4. closed-loop spatial multiplexing
5. multi-user MIMO
6. losed loop spatial multiplexing using a single transmission layer
7. beamforming
8. dual layer beamforming
9. eight-layer spatial multiplexing

In this thesis we always account for a single-antenna transmission, so for TM number 1.

2.6 ACCUMULATED MUTUAL INFORMATION

2.6.1 Shannon's coding theorem

A very important tool for the study of HARQ processes is the ACcumulated Mutual Information (ACMI). We first need to recall one of the fundamental theorems of information theory: the Shannon theorem on channel coding.

Theorem 2 (Shannon's channel coding theorem)**.** *Let us define the* information rate

$$R \triangleq \frac{\log_2 M}{n} \text{ [bit/channel use]}$$

where M *is the cardinality of the symbol alphabet and* n *the size of the codewords at the input of the channel, and the* capacity *of the channel*

$$C \triangleq \max I(x;y)$$

where $I(x;y)$ *is the mutual information between the input and the output of the channel. Then, for rates* $R < C$ *and* n *sufficiently large there is an encoder/decoder procedure assuring a symbol error probability* P_e *as small as desired, i.e. to ensure reliable communications. If, instead,* $R \geqslant C$ *a reliable communication is not possible.*

Note that the information rate can be equivalently expressed in the following way

$$R = \frac{\log_2 M}{n} = R_c \cdot \log_2 M \text{ [bit/channel use]}$$

recalling that R_c is the code rate of the transmitted message and M is the cardinality of the set of symbols, which depends on the type of modulation scheme that is applied.

2.6.2 What is Accumulated Mutual Information?

After having recalled the Shannon theorem, we can define the ACMI $I_\star(\boldsymbol{\gamma})$ straighforward: it is a way of increasing the capacity of the channel through a retransmission process.

SETTING Let $\mathbf{x}$ be a codeword of fixed length N bits, produced by an input sequence $\mathbf{u}$ of N_b bits; divide it in B sub-codewords $\mathbf{x} = (\mathbf{x}_1, \ldots, \mathbf{x}_B)$ of lengths $N_s \triangleq N/B$. Thus each subcodeword may be seen as a result of a coding procedure with rate

$$R_c = \frac{N_b}{N_s} = \frac{N_b}{N/B} = B \cdot \frac{N_b}{N}$$

where N_b/N is the code rate of the original codeword $\mathbf{x}$.

DEFINITION OF ACCUMULATED MUTUAL INFORMATION Depending on the kind of HARQ-type II employed, we provide a different definition for the ACMI $I_\star(\boldsymbol{\gamma})$, depending on the type of HARQ:

- In the case of CC-HARQ, we are increasing the resilience to channel noise so

$$I_\star^{CC}(\boldsymbol{\gamma}) \triangleq C\left(\sum_{i=1}^{m} \gamma_i\right)$$

- For IR-HARQ, instead, we are sending adding redundancy at every transmission attempt so

$$I_{\star}^{IR}(\boldsymbol{\gamma}) \triangleq \sum_{i=1}^{m} C(\gamma_i)$$

where m is the index of the last transmission attempt carried out.

In particular, the expression provided for the incremental redundancy approach is designed for a *parity priority* IR-HARQ. It is the most common incremental redundancy approach: at every transmission attempt one subcodeword from the entire original one is sent over the channel. However, in systematic codes, to ensure that every transmitted packet is self-decodable, each RV consists of the information bits and some new redundancy bits:

$$N_s = N_b + N_r$$

where $N_r = (N - N_b)/B$ is the fixed amount of new redundancy bits that is employed in every transmitted packet. At the receiver side the information part of the message is combined with its previously received versions, whereas the redundancy bits decrease the coding rate: in other words, the first ones experience a CC-HARQ and the second ones a IR-HARQ. This is the reasoning that stands behind the expression for the *systematic priority* ACMI:

$$I_{\star}^{IR,SP}(\boldsymbol{\gamma}) \triangleq R_c \cdot C\left(\sum_{i=1}^{m} \gamma_i\right) + (1 - R_c) \cdot \sum_{i=1}^{m} C(\gamma_i)$$

where

$$R_c = \frac{N_b}{N_b + N_r}$$

is the constant coding rate of each transmission.

In any case, the condition for ensuring reliable communications given by the Shannon's theorem then becomes

$$I_{\star}(\boldsymbol{\gamma}) < R = R_c \cdot \log_2 M = [M = 2] = R_c$$

See Caire and Tuninetti, 2001 for more details.

2.6.3 Variable-rate Incremental Redundancy

In the previous calculations, we have been assuming that the coding rate of each transmitted subcodeword is constant:

$$R_c = \frac{N_b}{N_s} = \text{const} < 1$$

However we can generalize the definition of ACMI in the case of a variable-rate IR-HARQ process (see Szczecinski *et al.*, 2010). Consider that each subcodeword has a different length of $N_{s,i}$ symbols of an alphabet of size M; then we have that

$$I_{\star}(\boldsymbol{\gamma}) = \frac{1}{\sum_{i=1}^{m} N_{s,i}} \sum_{i=1}^{m} C(\gamma_i) N_{s,i}$$

The condition from the Shannon theorem to provide a reliable communication becomes

$$I_{\star}(\boldsymbol{\gamma}) < \frac{N_b}{\sum_{i=1}^{m} N_{s,i}} \cdot \log_2 M$$

or in an equivalent way

$$\sum_{i=1}^{m} C(\gamma_i)\frac{N_{s,i}}{N_b} = \sum_{i=1}^{m} \frac{C(\gamma_i)}{R_{c,i}} < \log_2 M$$

where $R_{c,i}$ is the coding rate of the i-th transmitted packet.

Note that, in case we have $N_{s,i} = N_{s,j}\ \forall i, j$, it follows that $R_{c,i} = R_c$ and so we have

$$I_\star(\boldsymbol{\gamma}) = \sum_{i=1}^{m} C(\gamma_i)$$

and the condition of Shannon's channel coding theorem is the same we introduced at the beginning

$$I_\star(\boldsymbol{\gamma}) = \sum_{i=1}^{m} C(\gamma_i) < R_c \cdot \log_2 M$$

2.7 NOTATION DISCLAIMER

Note the differences in the notation in the following cases:

- *code rate*

  $$R_c = \frac{N_b}{N_s}$$

  It is the constant code rate of a packet and it is defined as the ratio between the amount of information bits N_b and total number of bits in the packet N_s.

- *code rate* of the m-th transmitted block

  $$R_{c,m} = \frac{N_b}{N_{s,m}}$$

  It is the coding rate of m-th transmitted packet in the case of variable rate transmission.

- *effective code rate (considering bit repetition)*

  $$R_{c,\mathrm{REP}}^{(m)} = \frac{N_b}{\sum_{i=1}^{m} N_{s,i}}$$

  It is the effective coding rate we obtain combining the first m-th transmitted packets at the receiver, considering all the transmitted packets.

- *effective code rate (without considering bit repetition)*

  $$R_c^{(m)} = \frac{N_b}{\sum_{i=1}^{l} N_{s,i}},\ 1 \leqslant l \leqslant m$$

  It is the effective coding rate we obtain combining the first m-th transmitted packets at the receiver, considering only the l packets which are not repeated.

Note that the relation between effective code rate considering bit repetition and without considering bit repetition is

$$R_c^{(m)} = \max\left\{R_{c,\mathrm{REP}}^{(m)}\,;\frac{1}{3}\right\}$$

3 PROPOSED SOLUTION

In this Chapter we propose a theoretical approach to model the HARQ process in LTE and evaluate the system performances; then we explain how to modify the model to account for the proposed Bayesian approach.

3.1 ASSUMPTIONS AND PARAMETERS

Let us consider a scenario which consists of one eNB and one UE. The downlink transmission involves the information transfer from the eNB, which is the source of the communication, towards the UE, which is the destination; the uplink transmission goes in the opposite direction, from the UE to the eNB. We will consider the uplink for the transmission of information, whereas the downlink for our purposes is simply a *feedback channel*. We make the following assumptions:

- the feedback channel is instantaneous and error-free,
- the probability of undetected errors and the probability of detecting an error while decoding is successful is 0,
- queues are always full, i.e., the source has always packets to transmit (*heavy traffic assumption*).

From a more technical point of view, we will assume to use a FDD technique, employing the paired[1] frequency band for Europe and Asia

$$B = [1920, 1980] \text{ MHz} \, , \mathcal{B} = 60 \text{ MHz}$$

Assuming that the first operator takes the first 20 MHz (equivalent to 100 RBs of 180 KHz) of this band, the center frequency is

$$f_c = 1930 \text{ MHz}$$

which is equivalent to a wavelenght

$$\lambda = \frac{c}{f_c} = 0.1553 \text{ m}$$

where

$$c \simeq 2.99 \cdot 10^8 \text{ m/s}$$

is the speed of light. Finally we recall the value of the TTI

$$\text{TTI} = 1 \text{ ms}$$

Since we will focus on a single HARQ process, recalling that the FDD in uplink employs 8 synchronized parallel HARQ processes, the time interval between subsequent transmission attempts is equal to

$$\tau = 8 \cdot \text{TTI} = 8 \text{ ms}$$

1 It means that the band is the same for both downlink and uplink transmissions.

We finally assume that the scheduler allocates always the same RB.

Note that the results will not depend on the choice of this particular carrier frequency: the impact of this parameter is just on the average speed of the terminal.

3.2 WIRELESS CHANNEL MODEL

We model the multipath fading of the radio channel using a *Rayleigh* distribution, assuming that the fading is constant accross the entire time interval τ. Therefore, the received signal in the n-th time interval τ Y_n is given by

$$Y_n = \sqrt{P_n} \cdot H_n \cdot X_n + Z_n$$

where $H_n \sim \text{Rayleigh}(\sigma)$, i.e., it has the following *probability density function* (pdf)

$$f_{|H_n|}(z) = \frac{z}{\sigma^2} \cdot e^{-z^2/(2\sigma^2)} \mathbb{1}(z)$$

and Z_n is a complex Additive White Gaussian Noise (AWGN), i.e.,

$$Z_n \sim \mathcal{CN}\left(0, \sigma_Z^2\right) \Leftrightarrow Z_n = Z_{n,I} + j \cdot Z_{n,Q}$$

$$Z_{n,I},\ Z_{n,Q} \sim \mathcal{N}\left(0, \frac{\sigma_Z^2}{2}\right)$$

$$Z_{n,I} \perp Z_{n,Q}$$

to account for the employed passband modulation. Note that, with the simple change of variable $z^2 = \xi$, $d\xi = 2\sqrt{\xi}\, dz$, the pdf becomes

$$f_{|H_n|^2}(\xi) = \frac{1}{2\sigma^2} \cdot e^{-\xi/(2\sigma^2)} \mathbb{1}(\xi)$$

Let us define the Signal to Interference plus Noise Ratio (SINR) as

$$\text{SINR} = \frac{\text{useful signal power}}{\text{interferers signal power} + \text{noise power}}$$

Since in our case of study no interferers are considered, the SINR coincides with the Signal to Noise Ratio (SNR):

$$\begin{aligned}
\gamma &= \frac{\text{useful signal power}}{\text{noise power}} = \\
&= \frac{P_{rx}}{N_0 B} = \\
&= \frac{P_{tx} \cdot G_{PL} \cdot |H_n|^2}{N_0 \mathcal{B}} = \\
&= \frac{P_{tx} \cdot G_{PL}}{N_0 \mathcal{B}} \cdot |H_n|^2 = \\
&= \gamma_0 \cdot |H_n|^2
\end{aligned}$$

where P_{tx} is the transmitted power, G_{PL} is the average path loss, N_0 is the noise power spectral density, $\mathcal{B}$ is the avaliable bandwidth and

$$\gamma_0 = \frac{P_{tx} \cdot G_{PL}}{N_0 \mathcal{B}}$$

is the average SNR. Since we don't consider power control and the distance between the transmitter and the receiver is fixed, γ_0 constant; therefore the uncertainty on the value of γ resides only in the multipath fading value

$$|H_n|^2 = \frac{\gamma}{\gamma_0}$$

If we include the average fading power into the path loss term γ_0 then we have

$$\mathbb{E}[|H_n|^2] = 2\sigma^2 = 1$$

and applying the change of variabile $\xi = \frac{\gamma}{\gamma_0}$, $d\xi = \frac{1}{\gamma_0}\, d\gamma$ then we obtain

$$f_\Gamma(\gamma) = \frac{1}{\gamma_0} \cdot e^{-\gamma/\gamma_0} \mathbb{1}(\gamma)$$

which is the SNR pdf in presence of Rayleigh multipath fading. The graphic representation of the pdf is shown in Figure 9.

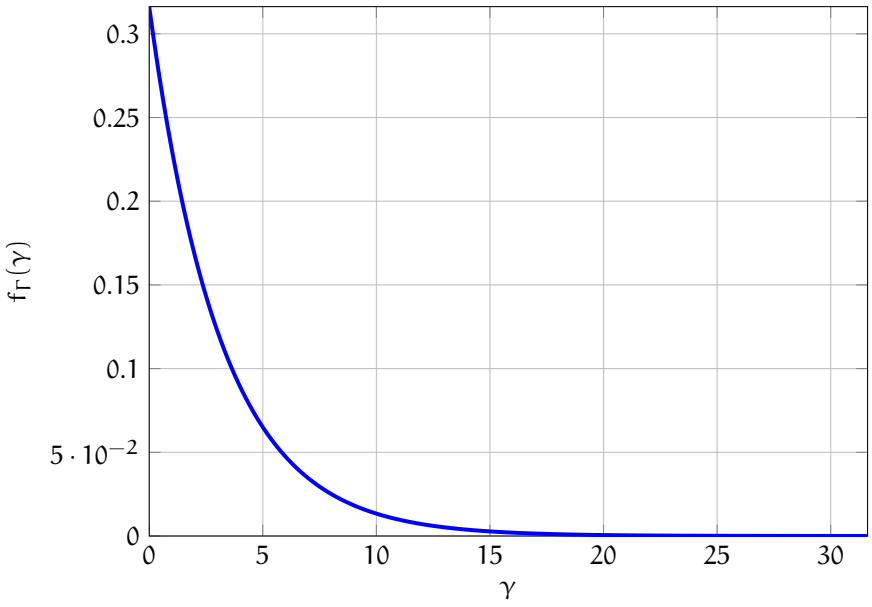

Figure 9: Probability density function of the signal-to-noise ratio in case of Rayleigh fading. In this picture the average SNR is equal to 5 dB.

3.3 CQI MODEL

As explained in Chapter 1, a very important parameter in the LTE cellular system is the Channel Quality Indicator (CQI), which represents a measurement of the channel state that is reported to the source (the UE) by the destination (the eNB), together with the acknowledgement or not-acknowledgement of the previouly transmitted packet and many other informations about the network and the system status. The source tunes the parameters of the next packet transmission according to the last CQI value in the case of uplink transmission.

According to Østerbø, 2011, numerical simulations show that the relationship between the CQI value and the actual SNR of the channel expressed in dB is a simple linear transformation:

$$\Gamma_{k,dB} = 10 \cdot \log_{10} \Gamma_k \triangleq k \cdot a + b$$

or equivalently

$$\Gamma_k \triangleq 10^{\frac{ka+b}{10}}$$

In LTE there exist $N = 15$ integer CQI values; the author of the cited article states that it is good practise to impose that

$$\begin{aligned} \Gamma_{1,dB} &= a + b \triangleq -6 \text{ dB} \\ \Gamma_{15,dB} &= 15a + b \triangleq 20 \text{ dB} \end{aligned}$$

getting

$$\begin{aligned} a &= 13/7 \\ b &= -55/7 \end{aligned}$$

Knowing a and b, it is possible to compute all the threshold values for the SNR Γ.

Note that this approach is in practise a *quantization* of the channel quality, where

$$\Gamma_{1,dB} = a + b \text{ and } \Gamma_{max,dB} \triangleq 20a + b$$

are the boundaries of the *granular region*, in which the quantization error is finite. Since we want to model the system for different average SNR values γ_0, we modify the proposed boundaries, imposing that

$$\begin{aligned} \Gamma_{1,dB} &= a + b = -30 \text{ dB} \\ \Gamma_{15,dB} &= 15a + b = 20 \text{ dB} \end{aligned}$$

and getting

$$\begin{aligned} a &= 25/7 \\ b &= -235/7 \end{aligned}$$

For what concerns the *reconstruction levels* $\overline{\Gamma}_k$ of such a quantization procedure, we recall from the theory of source coding that the optimal representative values of each interval are by definition the centroids of the decision regions, i.e.,

$$\begin{aligned} \overline{\Gamma_k} &\triangleq \int_{\Gamma_k}^{\Gamma_{k+1}} \gamma \cdot f_{\Gamma|\Gamma\in[\Gamma_k,\Gamma_{k+1}]}(\gamma|\gamma \in [\Gamma_k, \Gamma_{k+1}])\, d\gamma = \\ &= \frac{\int_{\Gamma_k}^{\Gamma_{k+1}} \gamma \cdot f_\Gamma(\gamma)\, d\gamma}{\int_{\Gamma_k}^{\Gamma_{k+1}} f_\Gamma(\gamma)\, d\gamma} \end{aligned}$$

In our theoretical model we will consider for sake of simplicity that the SNR can take values only in the finite set of the reconstruction levels, i.e.,

$$\gamma \in \{\overline{\Gamma_k}\}_{k=1,\dots,15}$$

Knowking the statistics of the SNR, we then compute the CQI stationary probabilities as

$$\pi_k \triangleq \mathbb{P}[CQI = k] = \mathbb{P}[\gamma \in [\Gamma_k, \Gamma_{k+1})] = \int_{\Gamma_k}^{\Gamma_{k+1}} f_\Gamma(\gamma)\, d\gamma \quad \forall k = 1, \dots, 14$$

and for CQI index $k = 15$ we consider

$$\mathbb{P}[CQI = 15] = \int_{\Gamma_{15}}^{\Gamma_{max}} f_\Gamma(\gamma)\, d\gamma$$

Table 2: SNR thresholds for the computation of the CQI by the receiver for an average SNR $\gamma_{0,dB}$ of 5 dB.

CQI k	$\Gamma_{k,dB}$	Γ_k	π_k	$\overline{\Gamma_k}$
1	−30.0000	0.0010	0.0004	0.0016
2	−26.4286	0.0023	0.0009	0.0037
3	−22.8571	0.0052	0.0021	0.0085
4	−19.2857	0.0118	0.0047	0.0193
5	−15.7143	0.0268	0.0107	0.0439
6	−12.1429	0.0611	0.0239	0.0998
7	−8.5714	0.1389	0.0522	0.2268
8	−5.0000	0.3162	0.1084	0.5137
9	−1.4286	0.7197	0.2008	1.1566
10	2.1429	1.6379	0.2882	2.5685
11	5.7143	3.7276	0.2394	5.5308
12	9.2857	8.4834	0.0662	11.2807
13	12.8571	19.3070	0.0022	22.4591
14	16.4286	43.9397	0.0000	47.1020
15	20.0000	100.0000	0.0000	103.1623

in such a way that

$$\sum_{k=1}^{15} \mathbb{P}[CQI = k] = \int_{\Gamma_1}^{\Gamma_{max}} f_\Gamma(\gamma)\, d\gamma = 1$$

since the design of the boundaries of the granular region Γ_1 and Γ_{max} is good enough.

An example of a set of values for the probabilities π_k for an average SNR $\gamma_{0,dB}$ of 5 dB can be found in the Table 2 too and is graphically represented in Figure 11.

3.4 CHANNEL TRANSITIONS MODEL

The wireless channel we are considering may be either *slow fading*, i.e., the CQI index does not change much between subsequent time intervals τ, or *fast fading*, i.e., the CQI index may experience large variations among subsequent transmission attempts. We assess the *speed* of the time variations of the channel through the *maximum Doppler frequency* (also called *Doppler shift*) f_m of the channel:

- if $f_m < 15$ Hz then the channel can be considered slow fading
- if $f_m > 30$ Hz then the channel can be considered fast fading
- for $15 \leqslant f_m \leqslant 30$ Hz the channel has an *intermediate* behaviour.

Since by definition

$$f_m \triangleq \frac{v}{\lambda}$$

the considered Doppler shift accounts for a transmitter moving at an average speed

$$v = f_m \cdot \lambda$$

so the higher the Doppler shift is the faster the transmitter moves.

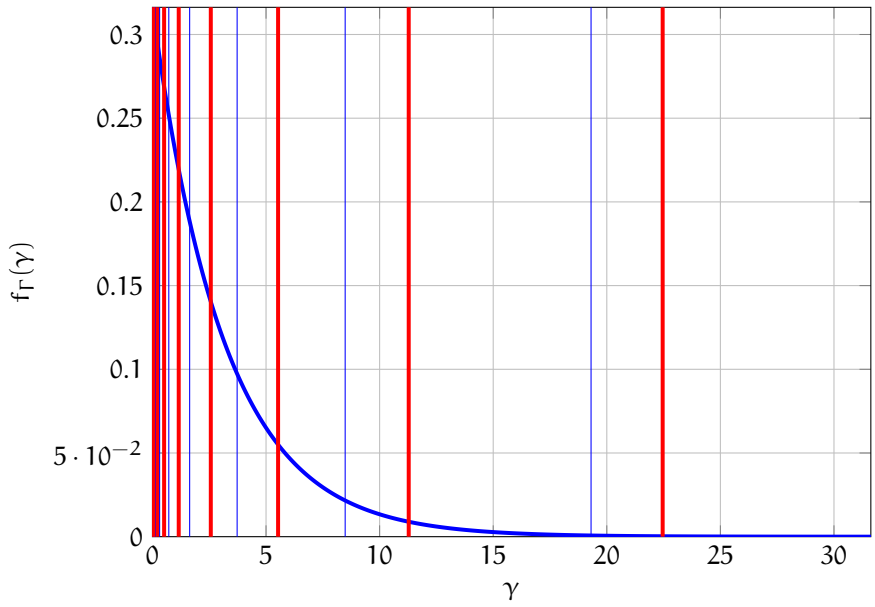

Figure 10: Example of Rayleigh fading channel quantization procedure. In this case the average SNR is 5 dB; the vertical blue lines indicate the boundaries of the decision regions (the CQI boundaries), whereas the vertical red ones indicate the reconstruction levels.

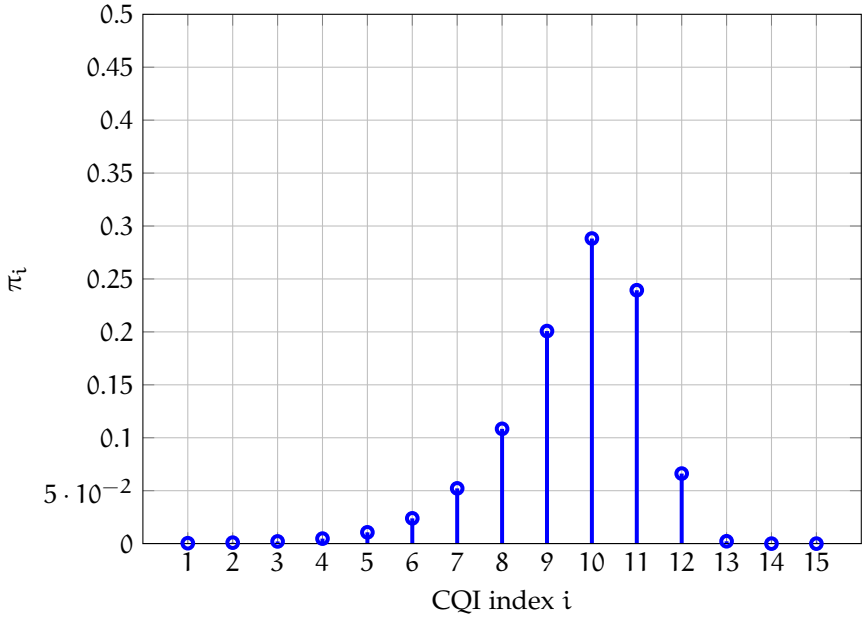

Figure 11: Example of stationary probabilities π_i of the wireless channel. The average SNR is $\gamma_{0,dB} = 5$ dB.

To characterize values of a Rayleigh fading channel at different time instants, we introduce the *bivariate Rayleigh pdf*:

$$f_{R_1,R_2}(r_1,r_2,r) = 4\frac{r_1 r_2}{1-r}\cdot e^{-\frac{r_1^2+r_2^2}{1-r}}\cdot I_0\left(\frac{2r_1 r_2}{1-r}\sqrt{r}\right)$$

where

- R_1 and R_2 are the random varibles associated to the two instants
- r_1, r_2 are the associated values of the fading envelope
- $I_0(x)$ is the *modified Bessel function of first type and order* 0:

$$I_0(x) \triangleq \frac{1}{\pi}\int_0^{\pi} e^{x\cos\theta}\,d\theta$$

- $r = \rho^2$, where ρ is the *Bessel function of first type and order* 0:

$$\rho \triangleq J_0(2\pi f_m \tau)$$

  Note that τ is the time displacement between the random variables, i.e., $\tau = 8\cdot \mathrm{TTI} = 8$ ms.

Recalling that

$$|H_n|^2 = \frac{\gamma}{\gamma_0}$$

we can compute the transition probabilities of the channel as

$$p_{i,j} = \mathbb{P}[j|i] = \frac{\mathbb{P}[i,j]}{\mathbb{P}[i]} = \frac{1}{\pi_i}\cdot\int_{\sqrt{\Gamma_i/\gamma_0}}^{\sqrt{\Gamma_{i+1}/\gamma_0}}\int_{\sqrt{\Gamma_j/\gamma_0}}^{\sqrt{\Gamma_{j+1}/\gamma_0}} f_{R_1,R_2}(r_1,r_2,r)\,dr_1 dr_2$$

An example of channel transition matrix we obtain for $\gamma_{0,\mathrm{dB}} = 5$ dB is reported in the Appendix A on page 43.

3.5 RATE MATCHING PROCESS MODEL

LTE employs a particular kind of rate matching process, which is difficult to characterize from an analytical point of view, since it is a mix of IR-HARQ and CC-HARQ. According to Cheng, 2008, the LTE rate matching process has to extract from the circular buffer 4 different subsets, denoted by RV, of the codeword for different transmission attempts of a single packet. Given that the interleaver is well-designed, it is known that most of the Hamming weight for turbo codes resides in the parity bits: if eccessive puncturing is applied to them then the effective minimum distance of the punctured code degrades at high code rates. Therefore, a small amount of systematic bit puncturing has been proposed in literature. In the case of LTE rate matching process the fraction of punctured systematic bits is $1/16 \simeq 6\%$. The structure of the circular buffer can be graphically represented as in Figure 12. We denote

- X as the number of systematic bits
- T as the number of transmitted bits
- Y as the number of punctured bits

We recall the relation among these variables:

$$T \triangleq 3X - Y = (3-\eta)X$$

where $\eta \triangleq Y/X$ is the ratio between the punctured bits and the systematic bits. Observing Figure 12 we can note that:

- the size of the circular buffer is $3X$, since the mother code rate of the turbo code is $1/3$;
- the systematic bit stream starts at 0, whereas the interlaced parity streams instead at X, with a phase displacement of $\pi/3$;
- the different RVs start at $\frac{3X}{4}i + \frac{1}{16}X$, where i is the index of the RV, and ...
- they end at $\frac{3X}{4}i + T + \frac{1}{16}X = \frac{3X}{4}i + (3-\eta)X + \frac{1}{16}X$

Note that the RV start points divide the circular buffer into 4 sectors of the same size $3X/4$. Knowing the value of

$$T = (3-\eta)X = f(\eta)$$

we are able to determine in which one of the 4 sectors of the buffer the pattern ends up to be and how many loops we need to go through. In this way there can be found 7 distinct rate matching processes to describe all the possibilities in terms of CQI: the complete assignments of the CQI values to the models can be found in Table 3 and all the relationships for the different transmission attempts are reported in Appendix B on page 45. Note that if $\eta < 0$ it means that there are some repeated bits already in the first transmission attempt, i.e., $T = (3-\eta)X > 3X$ and the effective code rate considering the repeated bits is $R_{c,REP}^{(0)} < 1/3$.

Note, also, that if we consider both the RV start and end points then we can divide the circular buffer into 8 sectors of just 2 different sizes (due to the simmetry of the structure) that depend on the value of T. Note that, in those cases in which $3Xi/4 + T > 3X$ for some retransmission index $i \in \{0,1,2,3\}$, some sectors are transmitted more than once, experiencing different SNRs.

3.6 ENHANCED RATE CHARACTERIZATION

In Chapter 2 we already explained a method to characterize analytically the code rates for subsequent transmission attempts in LTE. We now propose an enhancement of that model to provide an exact code rate computation. The effective code rate after the i-th transmission attempt considering repeated bits can be computed as follows:

$$R_{c,REP}^{(i)} = \frac{\text{number of information bits that are sent till tx attempt } i}{\text{number of total bits that are sent till tx attempt } i} =$$

$$= \begin{cases} \dfrac{\frac{15}{16}X}{\frac{3X}{4}i + T} & \text{if } \dfrac{3X}{4}i + T < 3X - \dfrac{X}{16} \\ \dfrac{\frac{15}{16}X + \left[\frac{3X}{4}i + T - \left(3X - \frac{X}{16}\right)\right]}{\frac{3X}{4}i + T} & \text{if } 3X - \dfrac{X}{16} \leqslant \dfrac{3X}{4}i + T < 3X \\ \dfrac{X}{\frac{3X}{4}i + T} & \text{otherwise} \end{cases}$$

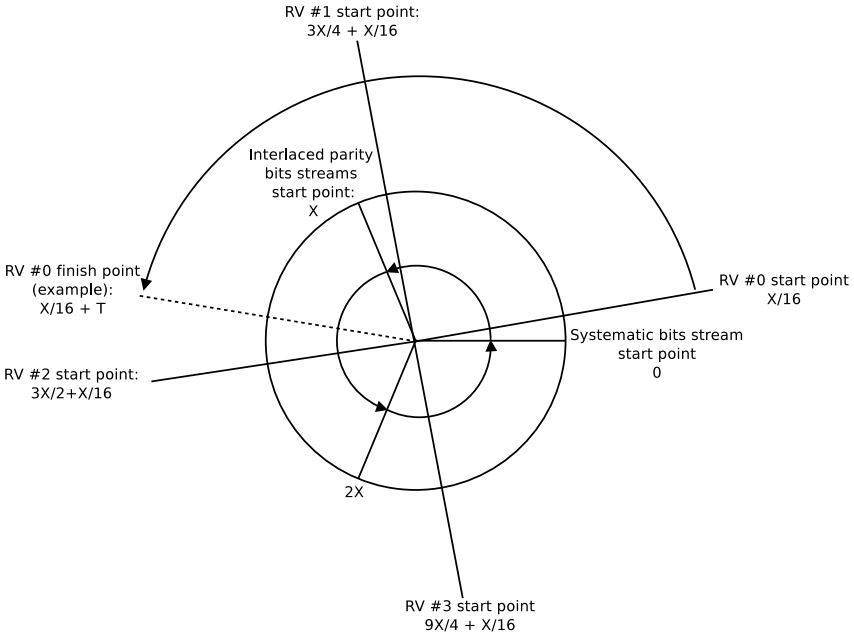

Figure 12: Representation of the virtual circular buffer employed during the bit selection procedure. Note the presence of a non-zero displaced starting position for the RV of index 0: this is done on purpose to maximize the turbo decoding procedure performances, which become poor in case of excessive parity bits punturing, especially for high code rates.

where $i \in \{0, 1, 2, 3\}$. We recall that

$$R_c^{(i)} = \max\left\{R_{c,\mathrm{REP}}^{(i)}\,;\frac{1}{3}\right\}$$

The new code rates obtained following this approach are reported in Table 3 and graphically represented in Figure 13.

The new values of η for all the CQI indexes can still be computed knowing the values of $R_{c,\mathrm{REP}}^{(0)}$, similarly to what has been done in Chapter 2; they can be found in Table 3.

3.7 HOW TO MODEL THE ACCUMULATED MUTUAL INFORMATION IN LTE?

Given the rate matcher characterization of the previous section, we can characterize the ACMI modeling a mixed Incremental Redundancy (IR) and Chase Combining (CC) HARQ:

$$I_\star(\boldsymbol{\gamma}) = \sum_{i=1}^{k} \lambda_i \cdot C\left(\sum_{j=1}^{m} \alpha_{ij}\gamma_j\right)$$

where

- $C(x) = \log_2(1+x)$ is the capacity of complex valued AWGN channel
- k is the number of sectors in which the circular buffer is partitioned, so it is $k = 8$

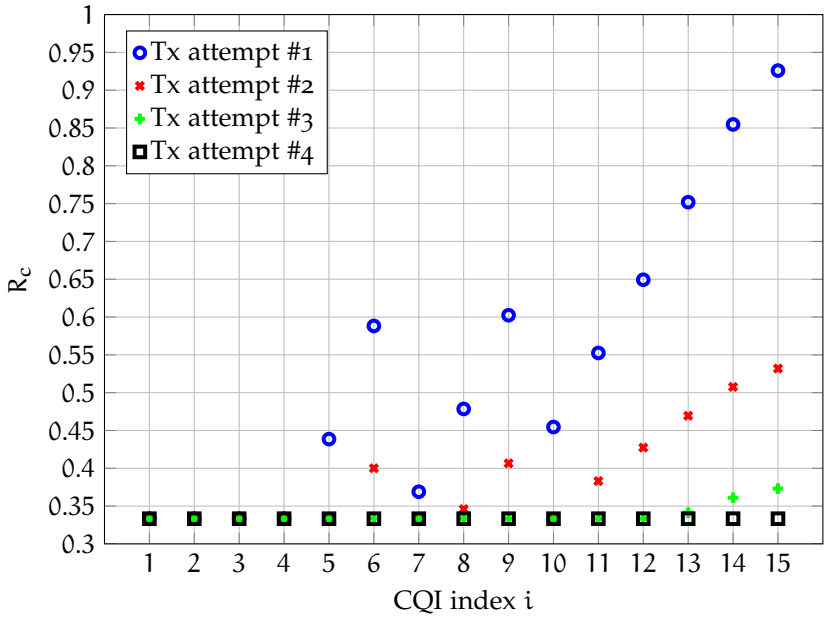

Figure 13: MCS for subsequent transmission attempts obtained using the enhanced approach. The coding rates are effective and compute without considering the repeated bits.

Table 3: The value of the puncturing patterns obtained using the enhanced solution are listed in column 3. In column 4 there can be found the mapping between CQI values and rate matcher models: depending on the position of η in the circular buffer, a different rate matcher model must be applied to characterize the ACMI.

CQI k	Modulation	η	$R_{c,REP}^{(0)}$	Rate matcher model
1	QPSK	−10.1300	0.076	#7
2	QPSK	−5.5300	0.12	#6
3	QPSK	−2.3100	0.19	#5
4	QPSK	−0.3200	0.30	#4
5	QPSK	0.8625	0.44	#2
6	QPSK	1.4062	0.59	#2
7	16-QAM	0.4594	0.37	#3
8	16-QAM	1.0406	0.48	#2
9	16-QAM	1.4438	0.60	#2
10	64-QAM	0.9375	0.45	#2
11	64-QAM	1.3031	0.55	#2
12	64-QAM	1.5562	0.65	#1
13	64-QAM	1.7531	0.75	#1
14	64-QAM	1.9031	0.85	#1
15	64-QAM	1.9875	0.93	#1

- $m \in \{1, 2, 3, 4\}$ is the transmission attempt index
- $\boldsymbol{\gamma} = [\gamma_1 \dots \gamma_m]^T$ is the vector that collects the SNR values that are experienced during the m subsequent transmission attempts
- α_{ij} is the number of times that sector i in the circular buffer experiences the SNR γ_j; it is
$$0 \leqslant \alpha_{ij} \leqslant m$$
- λ_i is the fraction of bits that belongs to sector i with respect to the total sent bits, without considering repeated bits. We always have that
$$\sum_{i=1}^{k} \lambda_i = 1$$

3.8 MARKOV CHAIN

To analyze the process of HARQ and rate matching we propose a Markov chain, which provides a good representation of the system. However we will evaluate the behaviour of the chain using numerical evaluations due to the complexity of such a model.

3.8.1 Structure of the chain

The states of the Markov chain we propose are triplets:

$$(K_n, X_n, CQI_n)$$

where

- $K_n \in \{0, 1, 2, 3, 4\}$ is the number of attempts done by the transmitter to deliver the current packet; if $K_n = 0$ it means that a new packet has just started its transmission round
- X_n is the value of the ACMI at the n-th transmission attempt; if $K_n = 0$ then it follows that $X_0 \triangleq 0$
- CQI_n is the CQI index experienced during the n-th transmission attempt; if $K_n = 0$ then CQI_n is just the CQI value of the previous packet last transmission attempt and it is used to select the appropriate MCS for the next packet transmission.

The total number of states is upper bounded by $15^5 = 759375$, but, since in many cases it is not possible to reach all other states from any state of the channel, the cardinality of the set of states is in practise

$$|\mathcal{S}| \ll 15^5$$

3.8.2 Rewards

We distinguish between two kinds of rewards:

1. $\mathcal{R}$ is the number of information bits which have been delivered at the end of a transmission round of a certain packet. We have that
$$\mathcal{R} = \begin{cases} R_c^{(i)} \cdot \log_2 M & \text{if the } i\text{-th retx attempt is successful} \\ 0 & \text{if the } 3^{rd} \text{ retx attempt fails} \end{cases}$$

2. $\mathcal{T}$ is the delay introduced by the retransmission process. Since we are taking into account a *synchronous* HARQ process, the value of $\mathcal{T}$ is discrete: it is a multiple of $\tau \triangleq 8 \cdot \text{TTI}$. We have that

$$\mathcal{T} = \begin{cases} (i+1) \cdot \tau & \text{if the } i\text{-th retx attempt is successful} \\ 4 \cdot \tau & \text{if the } 3^{\text{rd}} \text{ retx attempt fails} \end{cases}$$

The complete characterization of the proposed Markov model is available in Appendix C on page 55.

3.9 THE BAYESIAN APPROACH

Our aim now is that of introducing some kind of knowledge from past states of the channel and try to predict the channel behaviour in order to improve system performances. Let's give an example: the transmitter has just experienced a generic quadruple of CQI values (a *path* of CQIs)

$$\text{CQI}_a \rightarrow \text{CQI}_b \rightarrow \text{CQI}_c \rightarrow \text{CQI}_d$$

where CQI_a is the CQI relative to the first transmission attempt and so it is the one that defines the modulation and coding schemes that has to be used. In this case the path length L is equal to 4, but in general we have that

$$1 \leqslant L \leqslant 4$$

where the two boundaries $L = 1$ and $L = 4$ correspond to the *best case*, in which the transmission is immediately successful, and the *worst case*, in which we employ all possible transmission attempts, respectively. Excluding the best case, in all other cases we encounter inefficiencies in terms of accumulated delay due to the retransmission process. In every case, the MCS for the transmission of the following packet is selected according to the value of CQI_d, discarding the information relative to the rest of the path.

Now, we want to gain advantage of the knowledge of the history of the previous transmission. To do so, in those cases in which the previous transmission required at least one retransmission, i.e., $L \geqslant 2$, we let the transmitter compute the average value of the CQI experienced during the last packet delivery as

$$\overline{\text{CQI}} \triangleq \frac{1}{L} \sum_{k=1}^{L} \text{CQI}_k$$

This is the *learning* phase of the Bayesian approach. Then the *planning* takes place:

- if $\lceil \overline{\text{CQI}} \rceil > \text{CQI}_d$ then we could think of trying to be more aggressive, employing the MCS defined by $\lceil \overline{\text{CQI}} \rceil$
- otherwise we proceed as usual and employ the MCS defined by CQI_d.

Finally the transmitter *acts*, using the appropriate MCS for the next transmission round.

4 PERFORMANCE EVALUATION

In this Chapter we show the results of the proposed model obtained via numerical evaluation. The behaviour of the Markov chain in the long term has been numerically evaluated using Matlab, simulating the channel transitions and the accumulation of the mutual information among subsequent transmissions.

4.1 SIMULATION PROCEDURE

Due to the complexity of the proposed Markov chain, its performances have been evaluated using a *discrete-time* simulation. Table 4 contains the parameters that have been used for the simulation.

We have considered an average SNR range of $[-10, 30]$ dB. The simulation consists of the following steps:

1. Start from the channel state relative to the CQI with the highest stationary probability $\pi_i^\star = \max_j\{\pi_j\}$.
2. Select the digital modulation order and the code rates for the entire transmission round of the packet (initial transmission and the 3 possible retransmissions) according to the current start state.
3. Select the appropriate rate matching model with respect to the current start state.
4. Perform the subsequent transmission attempts, evaluating the appropriate formula for the ACMI for each attempt.
5. Tune the next packet transmission round according to the last experienced CQI index (*default* procedure) or following the Bayesian approach (*enhanced* procedure).
6. Repeat from step 2. for a certain fixed number of packets.
7. Compute averages and confidence intervals.

Table 4: In this Table are reported the simulation parameters that have been used to evaluate the long term behaviour of the proposed Markov chain. These parameters guarantees that the confidence intervals are approximately equal to zero.

Parameter	Value
minimum $\gamma_{0,\mathrm{dB}}$	-10 dB
maximum $\gamma_{0,\mathrm{dB}}$	30 dB
Montecarlo simulations	50
number of generated packets	5000
TTI	0.001 s

4.1.1 Possible enhancements

A possible enhancement of the model could be that of generating a random SNR sample in every CQI interval: this can be done using the rejection method.

4.2 OBSERVATIONS

The results of the numerical evaluation of the system bahviour are shown in Figures 14, 15, 17, 18 and 19.

4.2.1 Trends

Two quantities have been considered:

THROUGHPUT The throughput is approximately equal to zero for low average SNR values and increases as the average SNR increase; we note that the throughput tends to saturate for high average SNR values.

DELAY The delivery delay is maximum for lower average SNR values and it decreases as the average SNR increase. It tends to saturate for high SNRs too.

4.2.2 Comparison with real simulators

The trend of the curves is expected and similar to the real simulators, like the Vienna simulator (see Blumenstein *et al.*, 2011).

4.2.3 Enhancement of the model: does it work?

It can be seen that the enhanced model guarantees a higher throughput while decreasing the delivery delay with respect to the default model. Indeed there is a gap between the standard approach and the intelligent one: the latter provides the same performances of the former for lower average SNR values. However the size of that gap depends on how much correlated the channel is. Indeed

- if the channel is *slow fading* (low Doppler frequency, $f_m \in [5, 20]$ Hz) then the gap is quite large
- if the channel is *fast fading* (high Doppler frequency, $f_m > 30$ Hz) then the gap is closed.

One can conclude, therefore, that applying this kind of intelligence is worth when the channel is correlated.

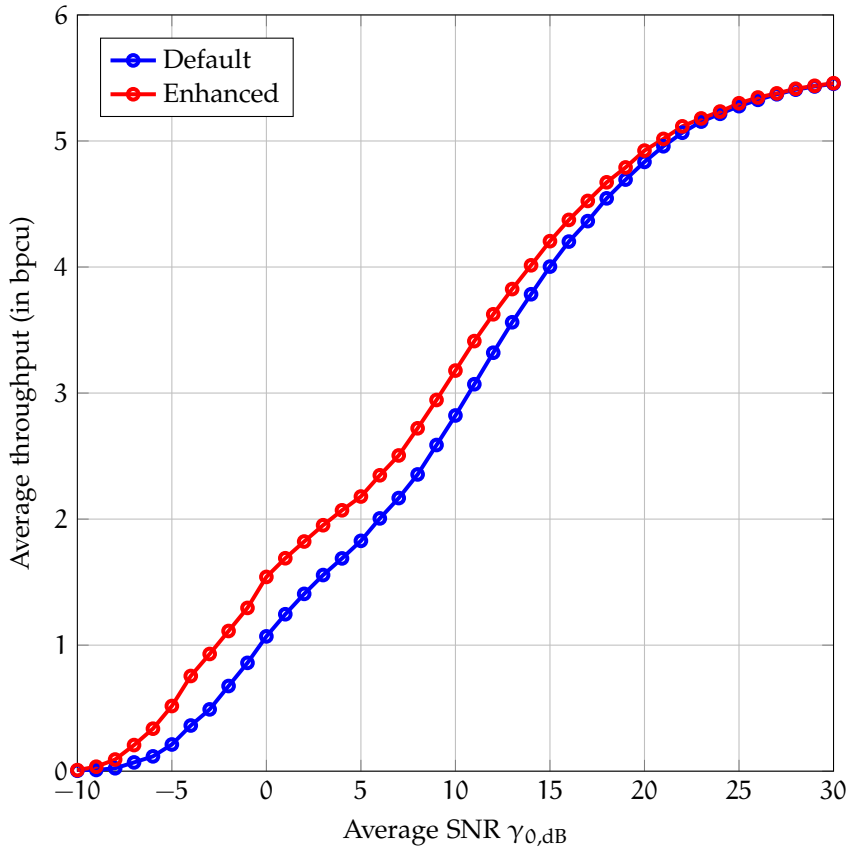

(a) Average throughput

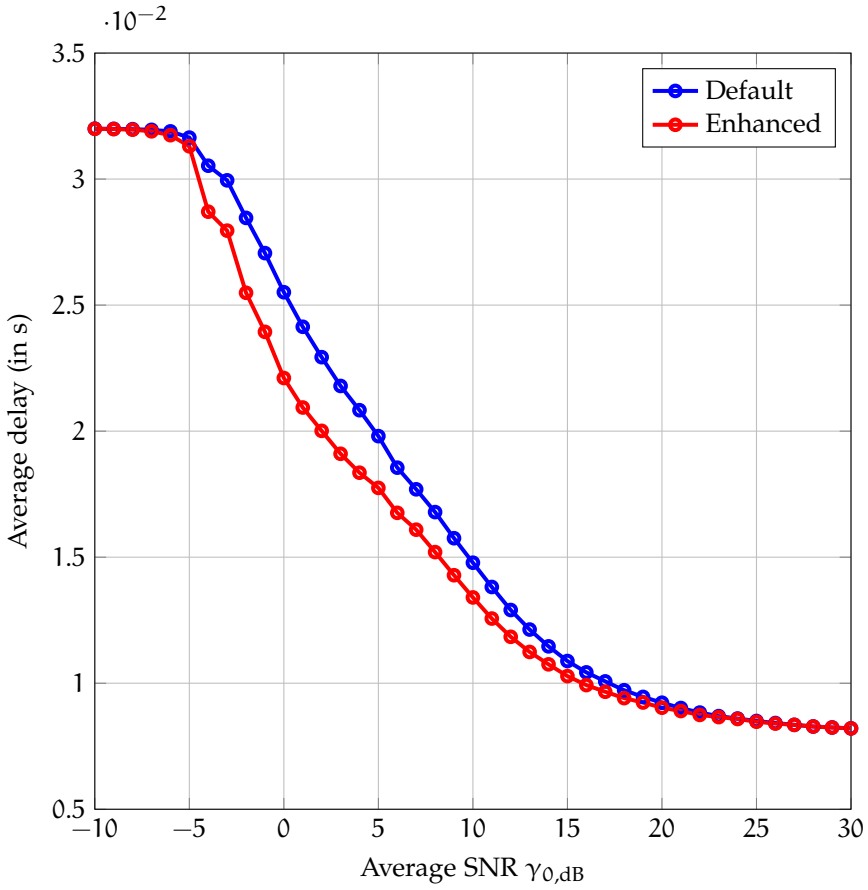

(b) Delivery delay

Figure 14: Performance results of the default and the enhanced HARQ process for $f_m = 5$ Hz.

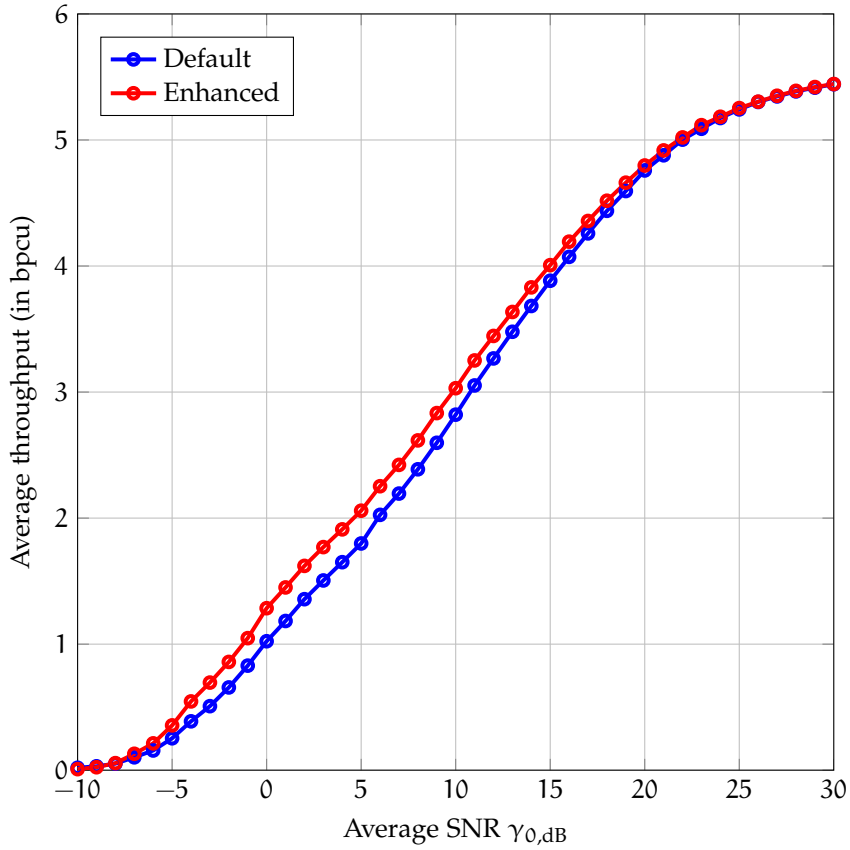

(a) Average throughput

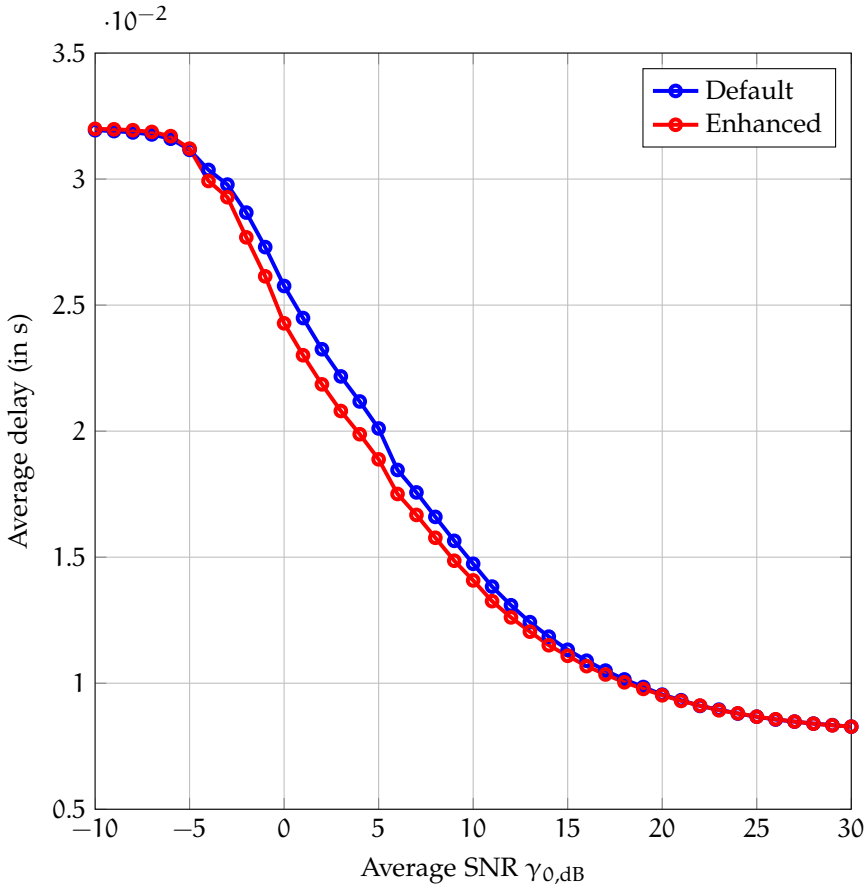

(b) Delivery delay

Figure 15: Performance results of the default and the enhanced HARQ process for $f_m = 10$ Hz.

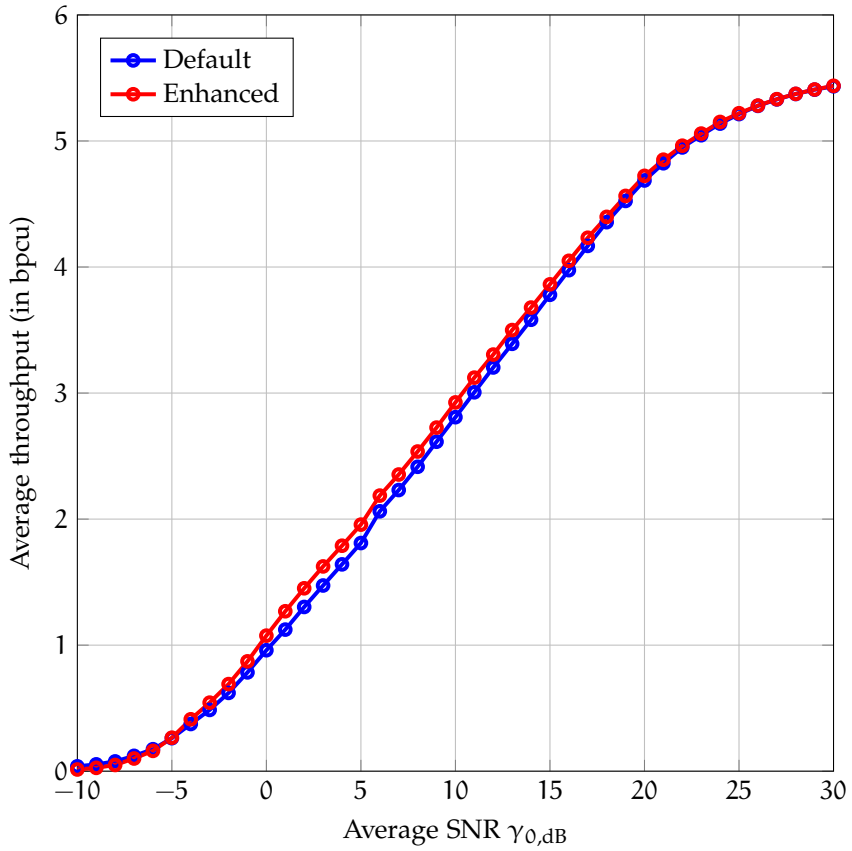

(a) Average throughput

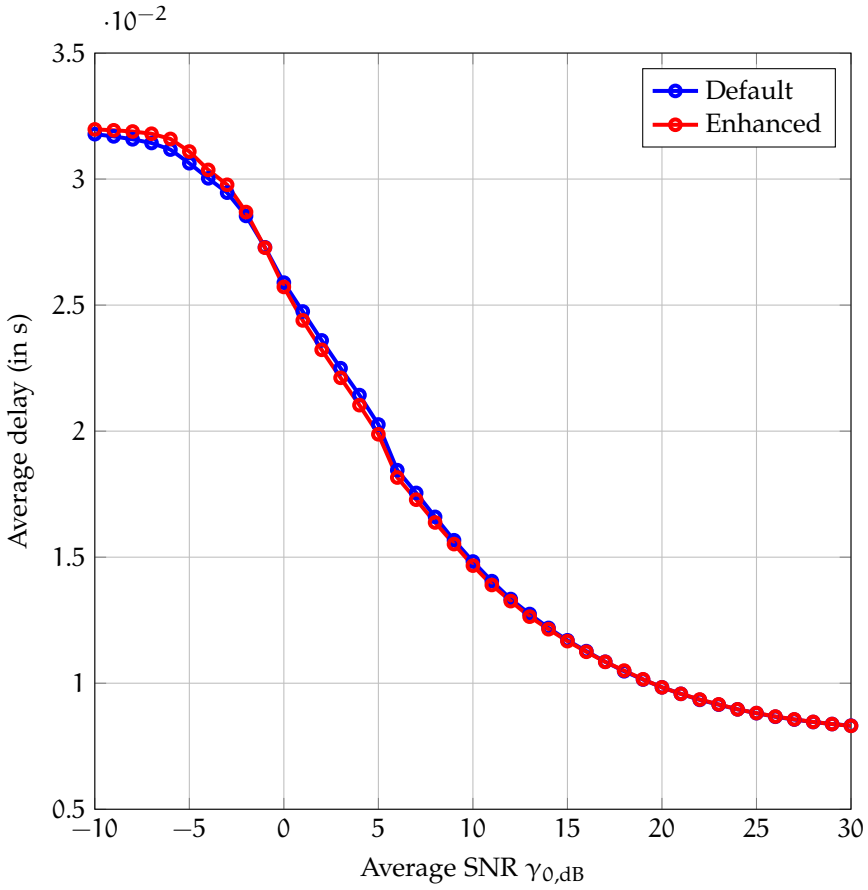

(b) Delivery delay

Figure 16: Performance results of the default and the enhanced HARQ process for $f_m = 15$ Hz.

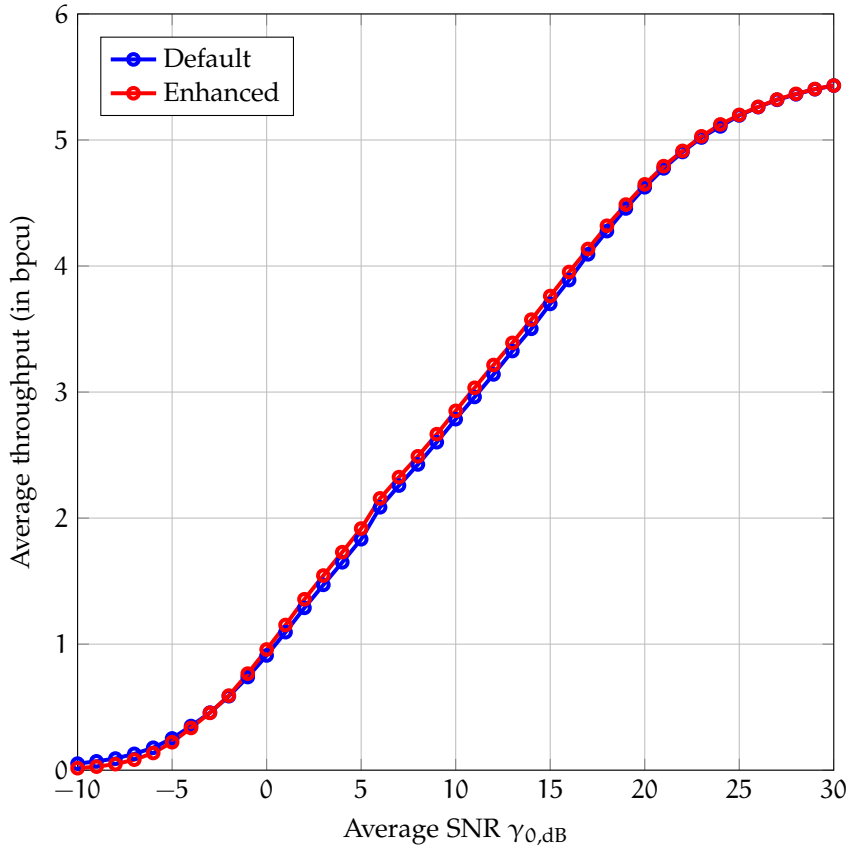

(a) Average throughput

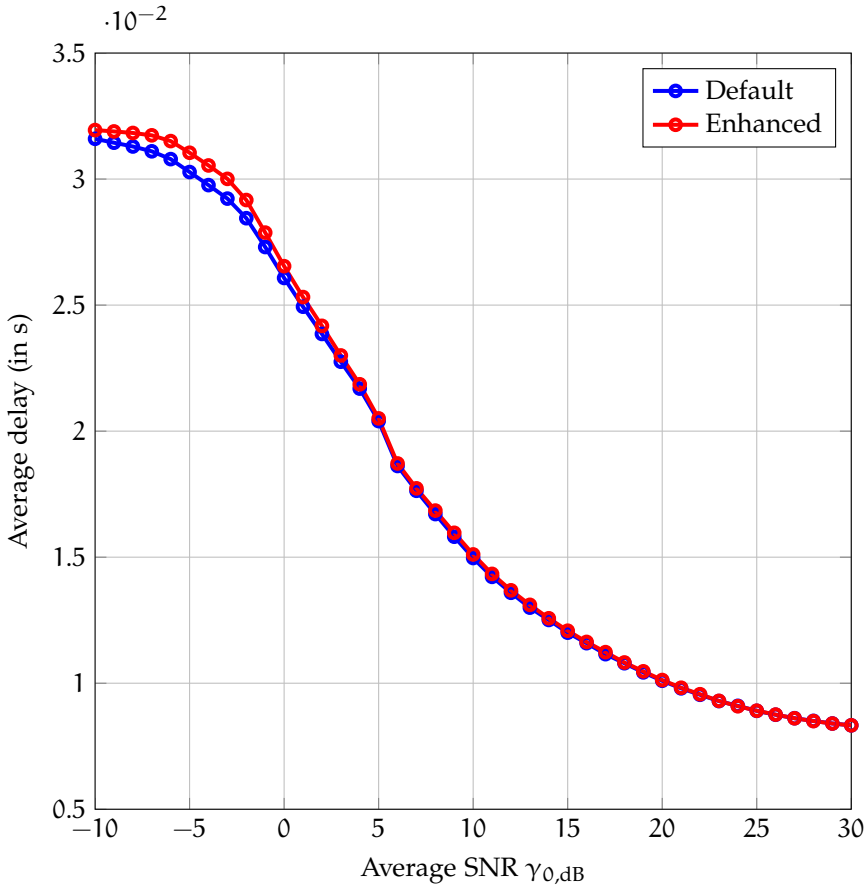

(b) Delivery delay

Figure 17: Performance results of the default and the enhanced HARQ process for $f_m = 20$ Hz.

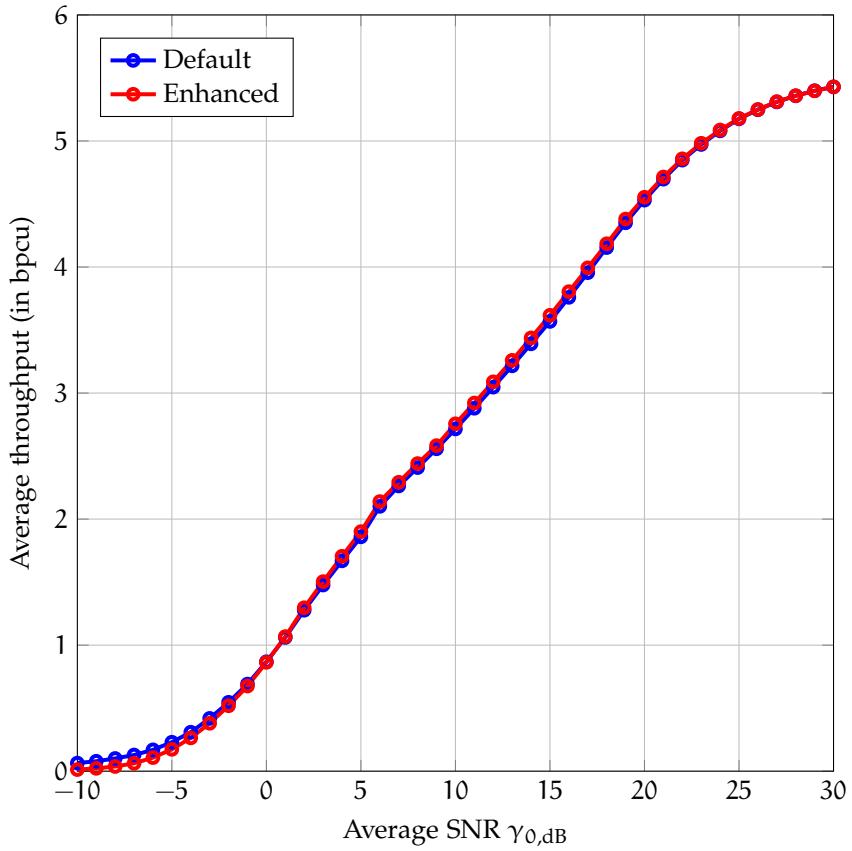

(a) Average throughput

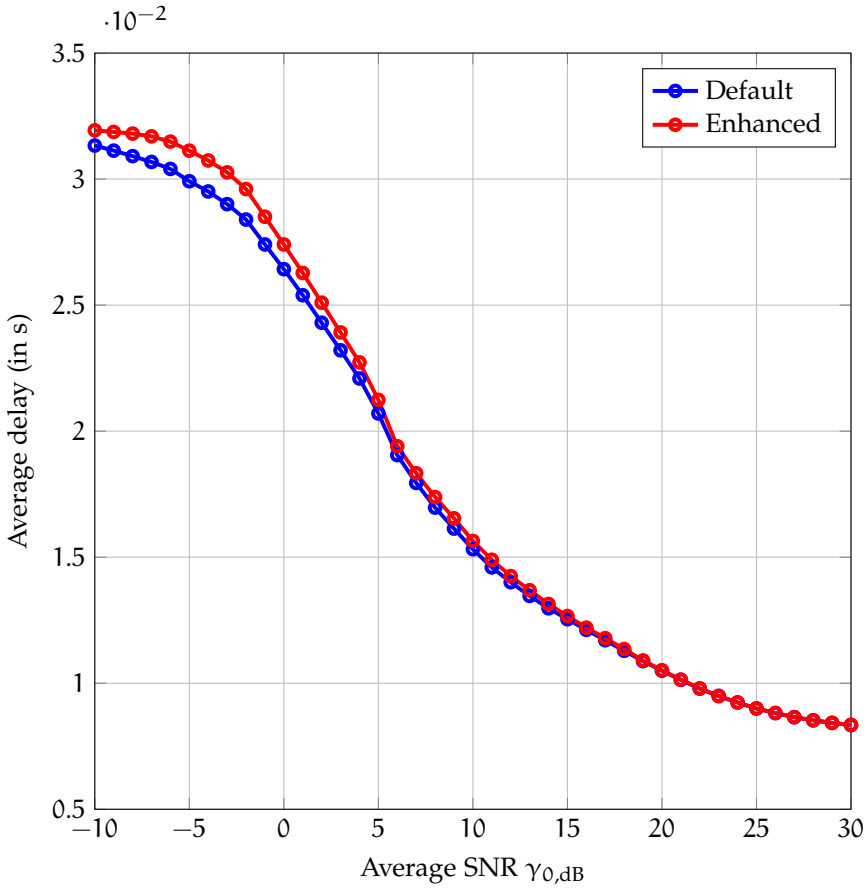

(b) Delivery delay

Figure 18: Performance results of the default and the enhanced HARQ process for $f_m = 30$ Hz.

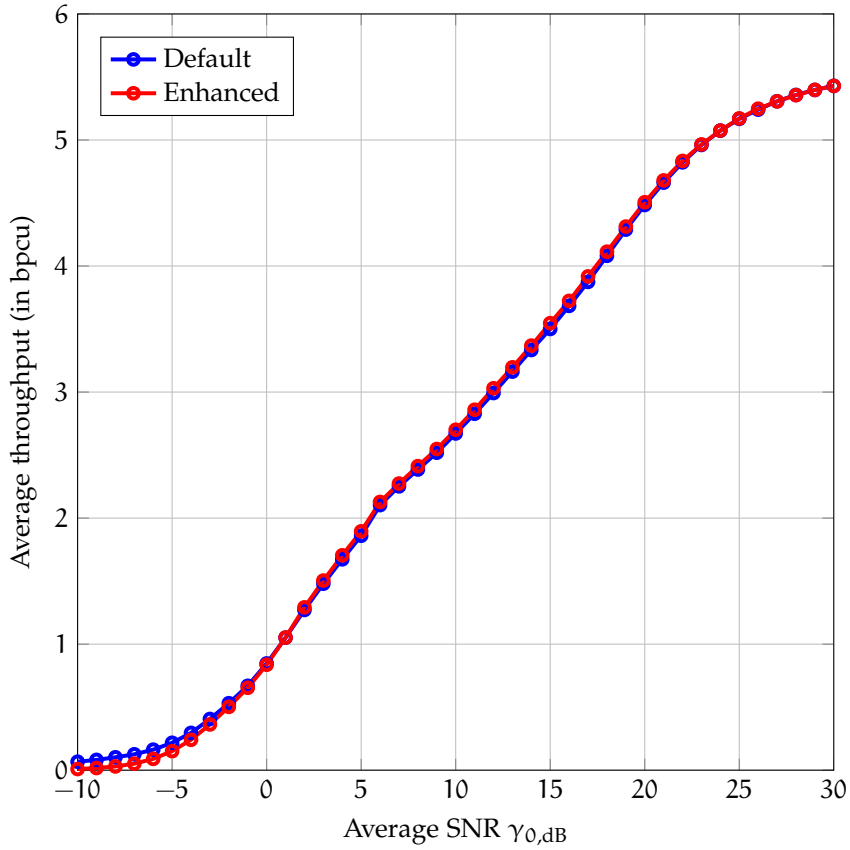

(a) Average throughput

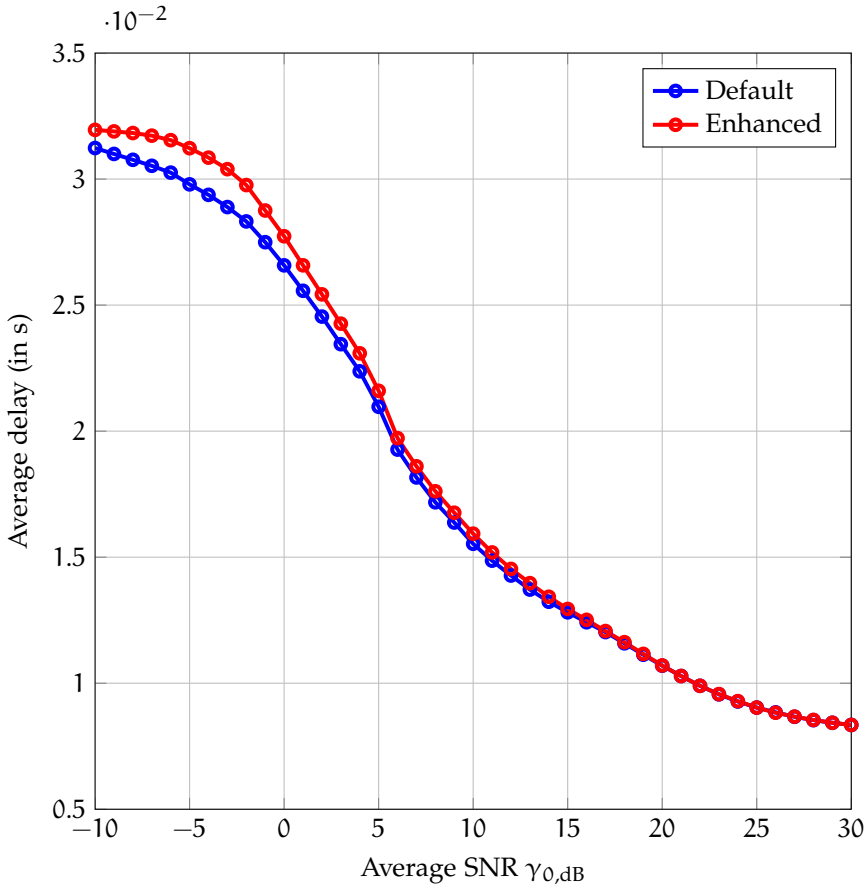

(b) Delivery delay

Figure 19: Performance results of the default and the enhanced HARQ process for $f_m = 40$ Hz.

5 CONCLUSION AND FUTURE WORK

In this thesis we propose a theoretical model based on Markov chains to study the Hybrid Automatic Repeat reQuest (HARQ) process of Long Term Evolution (LTE) cellular network technology. In particular, we have been focusing on a single HARQ process in the uplink channel: after a review of the state of the art, we first decided to account for a Rayleigh fading channel with Additive White Gaussian Noise (AWGN) noise; then we studied the rate matching process from an analytical point of view, introducing an expression of the ACcumulated Mutual Information (ACMI) taylored to the LTE rate matcher and designed a Markov model to evaluate the long term behaviour of the system. We also proposed a bayesian approach in which the system exploits the gathered information about the past channel states, trying to employ more aggressive Modulation and Coding Schemes (MCSs) when it is possible. Due to the complexity of such a model, the performances have been evaluated through numerical simulations: the results show that the proposed enhancement to the system provides an higher throughput and a lower delivery delay with respect to the default protocol for channels with low mobility.

Future works will include a further study of the enhanced system and the extension of the model to other kind of channels and to Multi-Input Multi-Output (MIMO).

CONCLUSIONI E SVILUPPI FUTURI

In questo elaborato viene proposto un modello di tipo Markoviano per studiare i processi di Hybrid Automatic Repeat reQuest (HARQ) impiegati nel sistema cellulare Long Term Evolution (LTE). In particolare ci siamo focalizzati su un singolo processo di HARQ nell'uplink: dopo aver esaminato lo stato dell'arte, si è deciso di considerare un canale con un'attenuazione di Rayleigh e rumore additivo gaussiano bianco (AWGN); quindi è stato analizzato il processo di rate matching, introducendo un'apposita espressione per l'informazione mutua accumulata (ACMI) per descriverne il comportamento; infine è stato proposto un modello di tipo Markoviano per valutare le prestazioni del sistema a lungo termine. É stato presentato, inoltre, un approccio di tipo bayesiano in cui il sistema sfrutta le informazioni raccolte sui precedenti stati del canale wireless, tentando di utilizzare modulazioni e rate di codifica più aggressivi quando possibile. A causa della complessità di tale modello, le prestazioni sono state valutate numericamente: i risultati dimostrano che il miglioramento proposto garantisce un maggiore throughput a fronte di un minor ritardo rispetto al protocollo predefinito per canali a bassa mobilità.

Gli sviluppi futuri comprendono uno studio approfondito del miglioramento apportato al sistema e l'estensione del modello ad altre tipologie di canale e al MIMO.

A CHANNEL TRANSITION MATRIX

In this Appendice we show an example of a transition matrix for the Rayleigh fading channel we have considered for our theoretical model. It has been computed numerically evaluating the *bivariate Rayleigh pdf*

$$f_{R_1,R_2}(r_1,r_2,r) = 4\frac{r_1 r_2}{1-r}\cdot e^{-\frac{r_1^2+r_2^2}{1-r}}\cdot I_0\left(\frac{2r_1 r_2}{1-r}\sqrt{r}\right)$$

where

- R_1 and R_2 are the random varibles associated to the two points
- r_1, r_2 are the associated values of the envelope
- $I_0(x)$ is the *modified Bessel function of first type and order* 0:

$$I_0(x) \triangleq \frac{1}{\pi}\int_0^{\pi} e^{x\cos\theta}\ d\theta$$

- $r = \rho^2$, where ρ is the *Bessel function of first type and order* 0:

$$\rho \triangleq J_0(2\pi f_m \tau)$$

- $f_m =$ Doppler shift
- $\tau = 8 \cdot \text{TTI} = 8$ ms

in the appropriate rectangular area $\left[\sqrt{\frac{\Gamma_i}{\gamma_0}}, \sqrt{\frac{\Gamma_{i+1}}{\gamma_0}}\right] \times \left[\sqrt{\frac{\Gamma_j}{\gamma_0}}, \sqrt{\frac{\Gamma_{j+1}}{\gamma_0}}\right]$, so that

$$p_{i,j} = \mathbb{P}[j|i] = \frac{\mathbb{P}[i,j]}{\mathbb{P}[i]} = \frac{1}{\pi_i}\cdot\int_{\sqrt{\Gamma_i/\gamma_0}}^{\sqrt{\Gamma_{i+1}/\gamma_0}}\int_{\sqrt{\Gamma_j/\gamma_0}}^{\sqrt{\Gamma_{j+1}/\gamma_0}} f_{R_1,R_2}(r_1,r_2,r)\ dr_1 dr_2$$

In this example we consider an average SNR $\gamma_{0,dB} = 5$ dB and a Doppler shift $f_m = 20$ Hz. Since we consider $f_c = 1930$ Hz, we have that the average speed of the transmitter is

$$v = \frac{f_m}{\lambda} = 3.1067 \text{ m/s} = 11.184 \text{ km/h}$$

The complete matrix can be found in the following page.

$$
P = \begin{bmatrix}
0.0010 & 0.0022 & 0.0050 & 0.0112 & 0.0250 & 0.0546 & 0.1130 & 0.2071 & 0.2907 & 0.2304 & 0.0581 & 0.0016 & 0.0000 & 0.0000 & 0.0000 \\
0.0010 & 0.0022 & 0.0050 & 0.0112 & 0.0250 & 0.0546 & 0.1129 & 0.2070 & 0.2907 & 0.2305 & 0.0583 & 0.0017 & 0.0000 & 0.0000 & 0.0000 \\
0.0010 & 0.0022 & 0.0050 & 0.0112 & 0.0250 & 0.0545 & 0.1127 & 0.2067 & 0.2906 & 0.2309 & 0.0586 & 0.0017 & 0.0000 & 0.0000 & 0.0000 \\
0.0010 & 0.0022 & 0.0049 & 0.0111 & 0.0249 & 0.0543 & 0.1123 & 0.2061 & 0.2904 & 0.2318 & 0.0594 & 0.0017 & 0.0000 & 0.0000 & 0.0000 \\
0.0009 & 0.0022 & 0.0049 & 0.0110 & 0.0246 & 0.0537 & 0.1113 & 0.2048 & 0.2899 & 0.2339 & 0.0611 & 0.0018 & 0.0000 & 0.0000 & 0.0000 \\
0.0009 & 0.0021 & 0.0048 & 0.0107 & 0.0240 & 0.0525 & 0.1090 & 0.2017 & 0.2887 & 0.2384 & 0.0650 & 0.0021 & 0.0000 & 0.0000 & 0.0000 \\
0.0009 & 0.0020 & 0.0045 & 0.0102 & 0.0228 & 0.0499 & 0.1041 & 0.1948 & 0.2859 & 0.2482 & 0.0740 & 0.0028 & 0.0000 & 0.0000 & 0.0000 \\
0.0008 & 0.0018 & 0.0040 & 0.0090 & 0.0202 & 0.0444 & 0.0938 & 0.1800 & 0.2788 & 0.2680 & 0.0947 & 0.0047 & 0.0000 & 0.0000 & 0.0000 \\
0.0006 & 0.0013 & 0.0030 & 0.0068 & 0.0154 & 0.0343 & 0.0743 & 0.1505 & 0.2593 & 0.3017 & 0.1422 & 0.0105 & 0.0000 & 0.0000 & 0.0000 \\
0.0003 & 0.0007 & 0.0017 & 0.0038 & 0.0087 & 0.0197 & 0.0449 & 0.1008 & 0.2101 & 0.3332 & 0.2437 & 0.0322 & 0.0001 & 0.0000 & 0.0000 \\
0.0001 & 0.0002 & 0.0005 & 0.0012 & 0.0027 & 0.0065 & 0.0161 & 0.0429 & 0.1193 & 0.2933 & 0.3970 & 0.1187 & 0.0015 & 0.0000 & 0.0000 \\
0.0000 & 0.0000 & 0.0001 & 0.0001 & 0.0003 & 0.0008 & 0.0022 & 0.0076 & 0.0317 & 0.1403 & 0.4295 & 0.3663 & 0.0211 & 0.0000 & 0.0000 \\
0.0000 & 0.0000 & 0.0000 & 0.0000 & 0.0000 & 0.0000 & 0.0000 & 0.0002 & 0.0013 & 0.0143 & 0.1569 & 0.6250 & 0.2019 & 0.0003 & 0.0000 \\
0.0000 & 0.0000 & 0.0000 & 0.0000 & 0.0000 & 0.0000 & 0.0000 & 0.0000 & 0.0000 & 0.0000 & 0.0018 & 0.1351 & 0.8093 & 0.0538 & 0.0000 \\
0.0000 & 0.0000 & 0.0000 & 0.0000 & 0.0000 & 0.0000 & 0.0000 & 0.0000 & 0.0000 & 0.0000 & 0.0000 & 0.0000 & 0.0779 & 0.9185 & 0.0036
\end{bmatrix}
$$

B RATE MATCHING MODELING AND ACMI

We recall briefly some notation:

- X = number of systematic bits
- $3X$ = size of the circular buffer
- $T = 3X - Y = (3 - \frac{Y}{X})X = (3 - \eta)X$ = number of sent bits
- Y = number of punctured bits
- $R_c^{(m-1)}$ = effective code rate after the m-th transmission, without considering repeated bits
- $R^{(m)}$ = information rate of the m-th transmission attempt

and the formula for the ACMI computation:

$$I_\star(\boldsymbol{\gamma}) = \sum_{i=1}^{k} \lambda_i \cdot C\left(\sum_{j=1}^{m} \alpha_{ij}\gamma_j\right)$$

where

- $C(x) = \log_2(1+x)$ is the capacity of complex valued AWGN channel
- k is the number of sectors in which the circular buffer is partitioned, so it is $k = 8$
- $m \in \{1, 2, 3, 4\}$ is the transmission attempt index
- $\boldsymbol{\gamma} = [\gamma_1 \dots \gamma_m]^T$ is the vector that collects the SNR values that are experienced during the m subsequent transmission attempts
- α_{ij} is the number of times that sector i in the circular buffer experiences the SNR γ_j; it is
$$0 \leqslant \alpha_{ij} \leqslant m$$
- λ_i is the fraction of bits that belongs to sector i with respect to the total sent bits, without considering repeated bits. We always have that
$$\sum_{i=1}^{k} \lambda_i = 1$$

B.1 RATE MATCHING #1

$$0 \leqslant T < \frac{3}{2}X$$

- **1st transmission attempt**

$$C(\gamma_1) \geqslant R^{(1)} = R_c^{(0)} \cdot \log_2 M$$

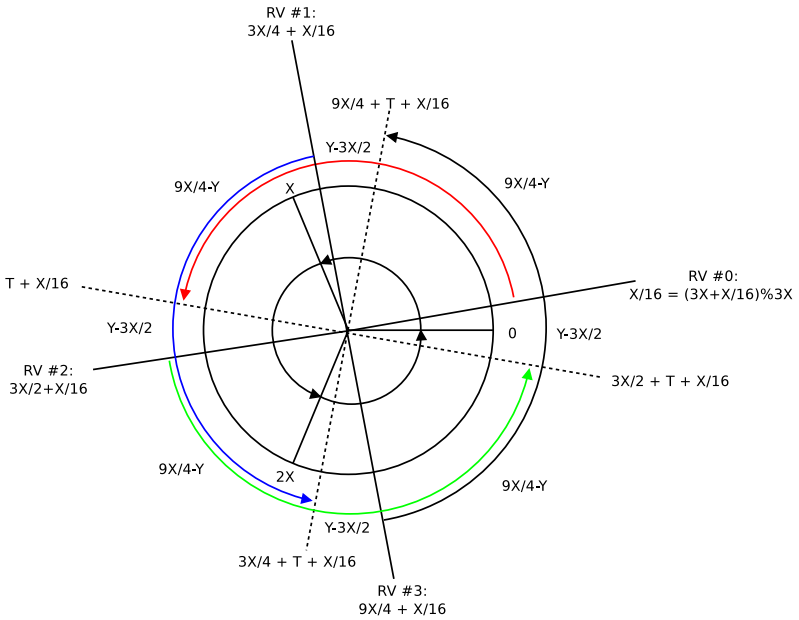

Figure 20: Graphical representation of the first type of rate matcher. The first transmission attempt is in red, the second in blue, the third in green and the fourth in black.

- **2nd transmission attempt**

$$\frac{3/4}{15/4-\eta}\cdot C(\gamma_1)+\frac{9/4-\eta}{15/4-\eta}\cdot C(\gamma_1+\gamma_2)+\frac{3/4}{15/4-\eta}\cdot C(\gamma_2)\gtrless R^{(2)}=R_c^{(1)}\cdot\log_2 M$$

- **3rd transmission attempt**

$$\begin{aligned}&\frac{3/4}{9/2-\eta}\cdot C(\gamma_1)+\frac{9/4-\eta}{9/2-\eta}\cdot C(\gamma_1+\gamma_2)+\frac{\eta-3/2}{9/2-\eta}\cdot C(\gamma_2)+\\&+\frac{9/4-\eta}{9/2-\eta}\cdot C(\gamma_2+\gamma_3)+\frac{3/4}{9/2-\eta}\cdot C(\gamma_3)\gtrless R^{(3)}=R_c^{(2)}\cdot\log_2 M\end{aligned}$$

- **4th transmission attempt**

$$\begin{aligned}&\frac{9/4-\eta}{3}\cdot C(\gamma_1+\gamma_4)+\frac{\eta-3/2}{3}\cdot C(\gamma_1)+\frac{9/4-\eta}{3}\cdot C(\gamma_1+\gamma_2)+\\&+\frac{\eta-3/2}{3}\cdot C(\gamma_2)+\frac{9/4-\eta}{3}\cdot C(\gamma_2+\gamma_3)+\frac{\eta-3/2}{3}\cdot C(\gamma_3)+\\&+\frac{9/4-\eta}{3}\cdot C(\gamma_3+\gamma_4)+\frac{\eta-3/2}{3}\cdot C(\gamma_4)\gtrless R^{(4)}=R_c^{(3)}\cdot\log_2 M\end{aligned}$$

B.2 RATE MATCHING #2

$$\frac{3}{2}X\leqslant T<\frac{9}{4}X$$

- **1st transmission attempt**

$$C(\gamma_1)\gtrless R^{(1)}$$

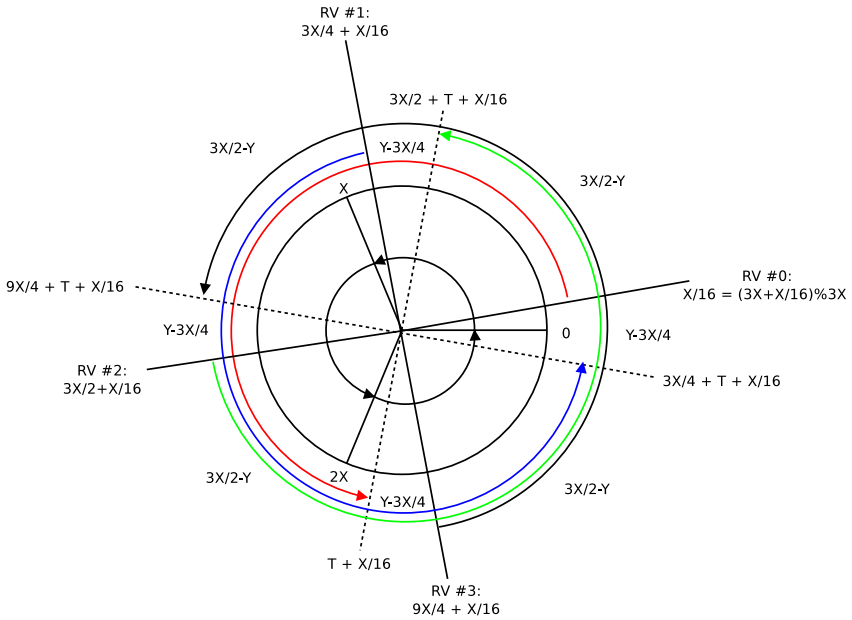

Figure 21: Graphical representation of the second type of rate matcher. The first transmission attempt is in red, the second in blue, the third in green and the fourth in black.

- **2nd transmission attempt**

$$\frac{3/4}{15/4-\eta}\cdot C(\gamma_1)+\frac{9/4-\eta}{15/4-\eta}\cdot C(\gamma_1+\gamma_2)+\frac{3/4}{15/4-\eta}\cdot C(\gamma_2)\gtrless R^{(2)}$$

- **3rd transmission attempt**

$$\frac{3/2-\eta}{3}\cdot C(\gamma_1+\gamma_3)+\frac{\eta-3/4}{3}\cdot C(\gamma_1)+\frac{3/4}{3}\cdot C(\gamma_1+\gamma_2)+$$
$$+\frac{3/2-\eta}{3}\cdot C(\gamma_1+\gamma_2+\gamma_3)+\frac{3/4}{3}\cdot C(\gamma_2+\gamma_3)+\frac{\eta-3/4}{3}\cdot C(\gamma_3)\gtrless R^{(3)}$$

- **4th transmission attempt**

$$\frac{3/2-\eta}{3}\cdot C(\gamma_1+\gamma_3+\gamma_4)+\frac{\eta-3/4}{3}\cdot C(\gamma_1+\gamma_4)+\frac{3/2-\eta}{3}\cdot C(\gamma_1+\gamma_2+\gamma_4)+$$
$$+\frac{\eta-3/4}{3}\cdot C(\gamma_1+\gamma_2)+\frac{3/2-\eta}{3}\cdot C(\gamma_1+\gamma_2+\gamma_3)+\frac{\eta-3/4}{3}\cdot C(\gamma_2+\gamma_3)+$$
$$+\frac{3/2-\eta}{3}\cdot C(\gamma_2+\gamma_3+\gamma_4)+\frac{\eta-3/4}{3}\cdot C(\gamma_3+\gamma_4)\gtrless R^{(4)}$$

B.3 RATE MATCHING #3

$$\frac{9}{4}X\leqslant T<3X$$

- **1st transmission attempt**

$$C(\gamma_1)\gtrless R^{(1)}$$

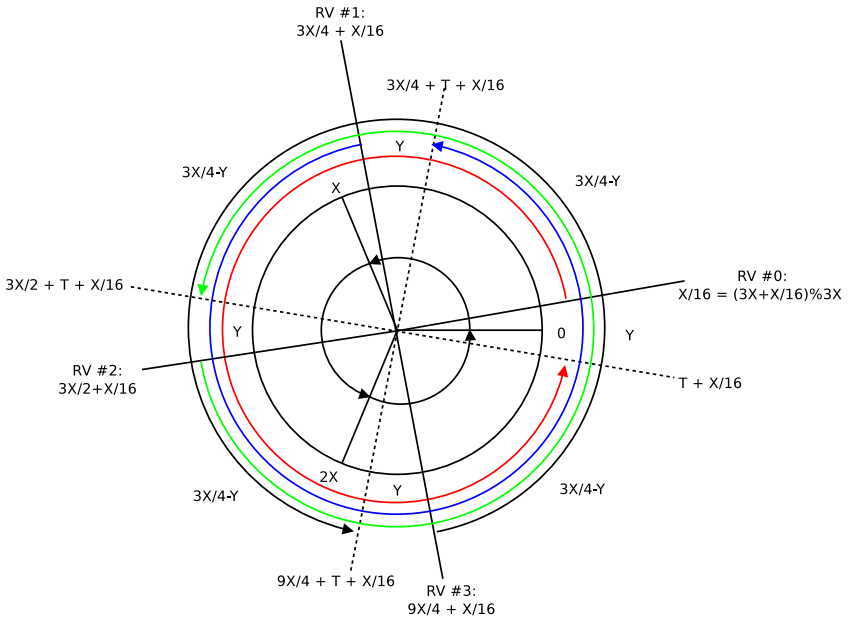

Figure 22: Graphical representation of the third type of rate matcher. The first transmission attempt is in red, the second in blue, the third in green and the fourth in black.

- **2nd transmission attempt**

$$\frac{3/4-\eta}{3}\cdot C(\gamma_1+\gamma_2)+\frac{\eta}{3}\cdot C(\gamma_1)+\frac{9/4-\eta}{3}\cdot C(\gamma_1+\gamma_2)+\frac{\eta}{3}\cdot C(\gamma_2)\geqslant R^{(2)}$$

- **3rd transmission attempt**

$$\frac{3/4-\eta}{3}\cdot C(\gamma_1+\gamma_2+\gamma_3)+\frac{\eta}{3}\cdot C(\gamma_1+\gamma_3)+\frac{3/4-\eta}{3}\cdot C(\gamma_1+\gamma_2+\gamma_3)+$$
$$+\frac{\eta}{3}\cdot C(\gamma_1+\gamma_2)+\frac{3/2-\eta}{3}\cdot C(\gamma_1+\gamma_2+\gamma_3)+\frac{\eta}{3}\cdot C(\gamma_2+\gamma_3)\geqslant R^{(3)}$$

- **4th transmission attempt**

$$\frac{3/4-\eta}{3}\cdot C(\gamma_1+\gamma_2+\gamma_3+\gamma_4)+\frac{\eta}{3}\cdot C(\gamma_1+\gamma_3+\gamma_4)+$$
$$+\frac{3/4-\eta}{3}\cdot C(\gamma_1+\gamma_2+\gamma_3+\gamma_4)+\frac{\eta}{3}\cdot C(\gamma_1+\gamma_2+\gamma_4)+$$
$$+\frac{3/4-\eta}{3}\cdot C(\gamma_1+\gamma_2+\gamma_3+\gamma_4)+\frac{\eta}{3}\cdot C(\gamma_1+\gamma_2+\gamma_3)+$$
$$+\frac{3/4-\eta}{3}\cdot C(\gamma_1+\gamma_2+\gamma_3+\gamma_4)+\frac{\eta}{3}\cdot C(\gamma_2+\gamma_3+\gamma_4)\geqslant R^{(4)}$$

B.4 RATE MATCHING #4

$$3X\leqslant T<3X+\frac{3}{4}X=\frac{15}{4}X$$

- **1st transmission attempt**

$$\frac{-\eta}{3}\cdot C(2\gamma_1)+\frac{3+\eta}{3}\cdot C(\gamma_1)\geqslant R^{(1)}$$

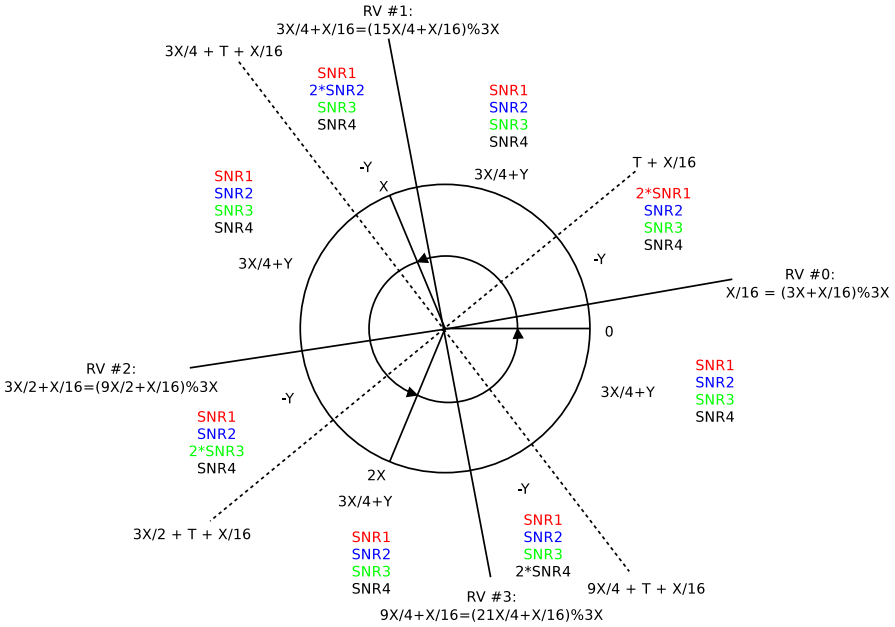

Figure 23: Graphical representation of the fourth type of rate matcher. The first transmission attempt is in red, the second in blue, the third in green and the fourth in black.

- **2nd transmission attempt**

$$\frac{-\eta}{3}\cdot C(2\gamma_1+\gamma_2)+\frac{3/4+\eta}{3}\cdot C(\gamma_1+\gamma_2)+$$
$$+\frac{-\eta}{3}\cdot C(\gamma_1+2\gamma_2)+\frac{9/4+\eta}{3}\cdot C(\gamma_1+\gamma_2)\geqslant R^{(2)}$$

- **3rd transmission attempt**

$$\frac{-\eta}{3}\cdot C(2\gamma_1+\gamma_2+\gamma_3)+\frac{3/4+\eta}{3}\cdot C(\gamma_1+\gamma_2+\gamma_3)+\frac{-\eta}{3}\cdot C(\gamma_1+2\gamma_2+\gamma_3)+$$
$$+\frac{3/4+\eta}{3}\cdot C(\gamma_1+\gamma_2+\gamma_3)+\frac{-\eta}{3}\cdot C(\gamma_1+\gamma_2+2\gamma_3)+\frac{3/2+\eta}{3}\cdot C(\gamma_1+\gamma_2+\gamma_3)\geqslant R^{(3)}$$

- **4th transmission attempt**

$$\frac{-\eta}{3}\cdot C(2\gamma_1+\gamma_2+\gamma_3+\gamma_4)+\frac{3/4+\eta}{3}\cdot C(\gamma_1+\gamma_2+\gamma_3+\gamma_4)+$$
$$+\frac{-\eta}{3}\cdot C(\gamma_1+2\gamma_2+\gamma_3+\gamma_4)+\frac{3/4+\eta}{3}\cdot C(\gamma_1+\gamma_2+\gamma_3+\gamma_4)+$$
$$+\frac{-\eta}{3}\cdot C(\gamma_1+\gamma_2+2\gamma_3+\gamma_4)+\frac{3/4+\eta}{3}\cdot C(\gamma_1+\gamma_2+\gamma_3+\gamma_4)+$$
$$+\frac{-\eta}{3}\cdot C(\gamma_1+\gamma_2+\gamma_3+2\gamma_4)+\frac{3/4+\eta}{3}\cdot C(\gamma_1+\gamma_2+\gamma_3+\gamma_4)\geqslant R^{(4)}$$

B.5 RATE MATCHING #5

$$3X+\frac{9}{4}X\leqslant T<6X$$

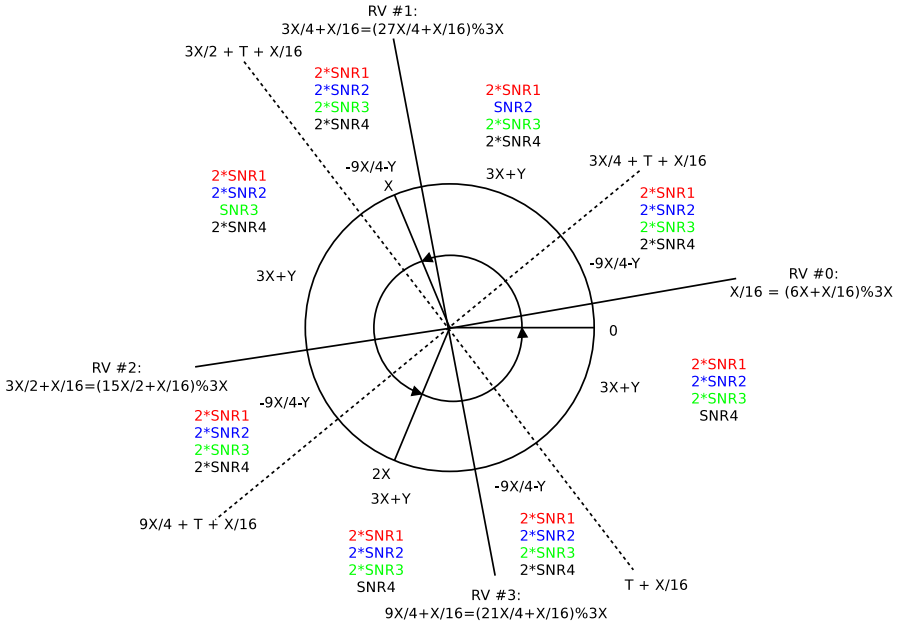

Figure 24: Graphical representation of the fifth type of rate matcher. The first transmission attempt is in red, the second in blue, the third in green and the fourth in black.

- **1st transmission attempt**

$$\frac{-\eta}{3}\cdot C(2\gamma_1)+\frac{3+\eta}{3}\cdot C(\gamma_1)\gtrless R^{(1)}$$

- **2nd transmission attempt**

$$\begin{aligned}&\frac{-\eta-9/4}{3}\cdot C(2\gamma_1+2\gamma_2)+\frac{3+\eta}{3}\cdot C(2\gamma_1+\gamma_2)+\\&+\frac{-3/4-\eta}{3}\cdot C(2\gamma_1+2\gamma_2)+\frac{3+\eta}{3}\cdot C(\gamma_1+2\gamma_2)\gtrless R^{(2)}\end{aligned}$$

- **3rd transmission attempt**

$$\begin{aligned}&\frac{-\eta-9/4}{3}\cdot C(2\gamma_1+2\gamma_2+2\gamma_3)+\frac{3+\eta}{3}\cdot C(2\gamma_1+\gamma_2+2\gamma_3)+\\&+\frac{-\eta-9/4}{3}\cdot C(2\gamma_1+2\gamma_2+2\gamma_3)+\frac{3+\eta}{3}\cdot C(2\gamma_1+2\gamma_2+\gamma_3)+\\&+\frac{-\eta-3/2}{3}\cdot C(2\gamma_1+2\gamma_2+2\gamma_3)+\frac{3+\eta}{3}\cdot C(\gamma_1+2\gamma_2+2\gamma_3)\gtrless R^{(3)}\end{aligned}$$

- **4th transmission attempt**

$$\begin{aligned}&\frac{-\eta-9/4}{3}\cdot C(2\gamma_1+2\gamma_2+2\gamma_3+2\gamma_4)+\frac{3+\eta}{3}\cdot C(2\gamma_1+\gamma_2+2\gamma_3+2\gamma_4)+\\&+\frac{-\eta-9/4}{3}\cdot C(2\gamma_1+2\gamma_2+2\gamma_3+2\gamma_4)+\frac{3+\eta}{3}\cdot C(2\gamma_1+2\gamma_2+\gamma_3+2\gamma_4)+\\&+\frac{-\eta-9/4}{3}\cdot C(2\gamma_1+2\gamma_2+2\gamma_3+2\gamma_4)+\frac{3+\eta}{3}\cdot C(2\gamma_1+2\gamma_2+2\gamma_3+\gamma_4)+\\&+\frac{-\eta-9/4}{3}\cdot C(2\gamma_1+2\gamma_2+2\gamma_3+2\gamma_4)+\frac{3+\eta}{3}\cdot C(\gamma_1+2\gamma_2+2\gamma_3+2\gamma_4)\gtrless R^{(4)}\end{aligned}$$

B.6 RATE MATCHING #6

$$6X + \frac{9}{4}X \leqslant T < 9X$$

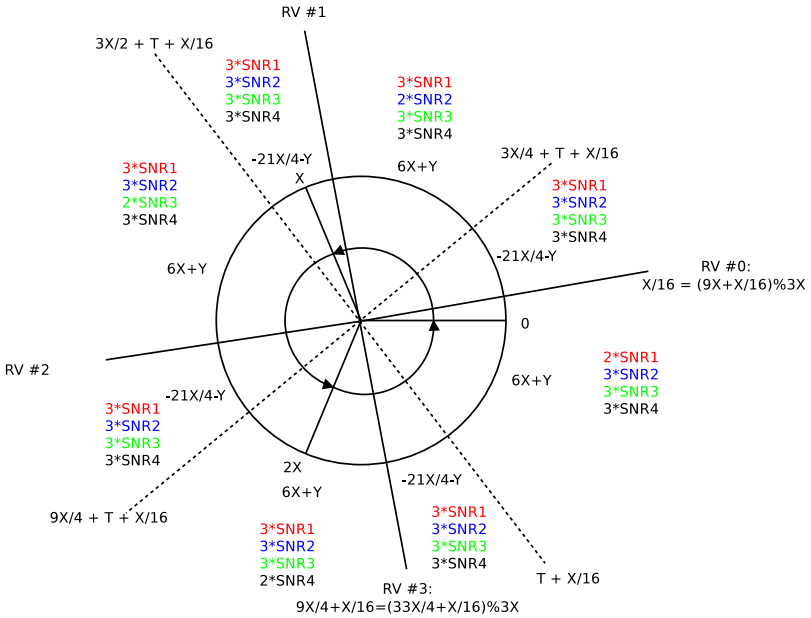

Figure 25: Graphical representation of the sixth type of rate matcher. The first transmission attempt is in red, the second in blue, the third in green and the fourth in black.

- **1st transmission attempt**

$$\frac{-\eta - 3}{3} \cdot C(3\gamma_1) + \frac{6+\eta}{3} \cdot C(2\gamma_1) \gtrless R^{(1)}$$

- **2nd transmission attempt**

$$\begin{aligned}&\frac{-\eta - 21/4}{3} \cdot C(3\gamma_1 + 3\gamma_2) + \frac{6+\eta}{3} \cdot C(3\gamma_1 + 2\gamma_2) + \\ &+ \frac{-15/4 - \eta}{3} \cdot C(3\gamma_1 + 3\gamma_2) + \frac{6+\eta}{3} \cdot C(2\gamma_1 + 3\gamma_2) \gtrless R^{(2)}\end{aligned}$$

- **3rd transmission attempt**

$$\begin{aligned}&\frac{-\eta - 21/4}{3} \cdot C(3\gamma_1 + 3\gamma_2 + 3\gamma_3) + \frac{6+\eta}{3} \cdot C(3\gamma_1 + 2\gamma_2 + 3\gamma_3) + \\ &+ \frac{-\eta - 21/4}{3} \cdot C(3\gamma_1 + 3\gamma_2 + 3\gamma_3) + \frac{6+\eta}{3} \cdot C(3\gamma_1 + 3\gamma_2 + 2\gamma_3) + \\ &+ \frac{-\eta - 9/2}{3} \cdot C(3\gamma_1 + 3\gamma_2 + 3\gamma_3) + \frac{6+\eta}{3} \cdot C(2\gamma_1 + 3\gamma_2 + 3\gamma_3) \gtrless R^{(3)}\end{aligned}$$

- **4th transmission attempt**

$$\frac{-\eta-21/4}{3}\cdot C(3\gamma_1+3\gamma_2+3\gamma_3+3\gamma_4)+\frac{6+\eta}{3}\cdot C(3\gamma_1+2\gamma_2+3\gamma_3+3\gamma_4)+$$
$$+\frac{-\eta-21/4}{3}\cdot C(3\gamma_1+3\gamma_2+3\gamma_3+3\gamma_4)+\frac{6+\eta}{3}\cdot C(3\gamma_1+3\gamma_2+2\gamma_3+3\gamma_4)+$$
$$+\frac{-\eta-21/4}{3}\cdot C(3\gamma_1+3\gamma_2+3\gamma_3+3\gamma_4)+\frac{6+\eta}{3}\cdot C(3\gamma_1+3\gamma_2+3\gamma_3+2\gamma_4)+$$
$$+\frac{-\eta-21/4}{3}\cdot C(3\gamma_1+3\gamma_2+3\gamma_3+3\gamma_4)+\frac{6+\eta}{3}\cdot C(2\gamma_1+3\gamma_2+3\gamma_3+3\gamma_4)\gtrless R^{(4)}$$

B.7 RATE MATCHING #7

$$12X+\frac{3}{4}X\leqslant T<12X+\frac{3}{2}X$$

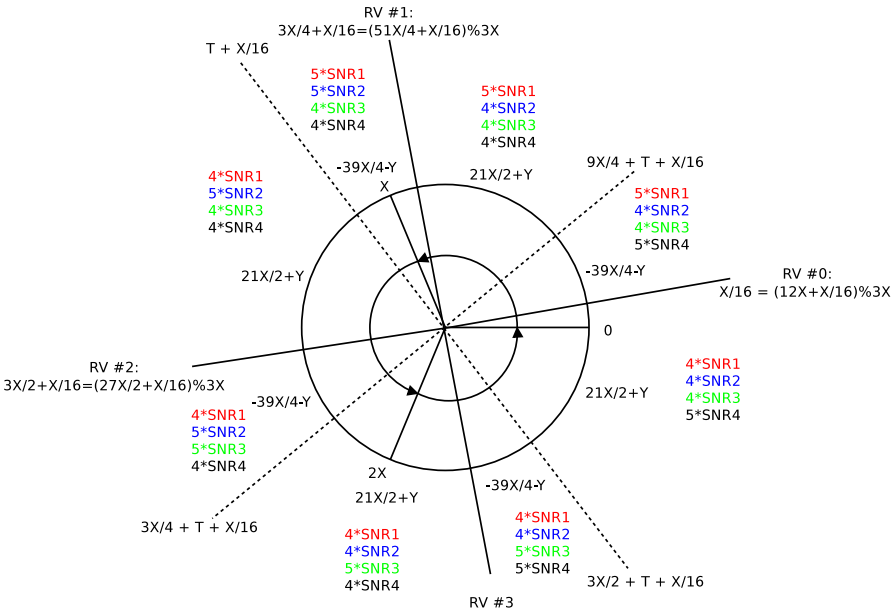

Figure 26: Graphical representation of the seventh type of rate matcher. The first transmission attempt is in red, the second in blue, the third in green and the fourth in black.

- **1st transmission attempt**

$$\frac{-\eta-9}{3}\cdot C(5\gamma_1)+\frac{12+\eta}{3}\cdot C(4\gamma_1)\gtrless R^{(1)}$$

- **2nd transmission attempt**

$$\frac{3/4}{3}\cdot C(5\gamma_1+4\gamma_2)+\frac{-\eta-39/4}{3}\cdot C(5\gamma_1+5\gamma_2)+$$
$$+\frac{3/4}{3}\cdot C(4\gamma_1+5\gamma_2)+\frac{45/4+\eta}{3}\cdot C(4\gamma_1+4\gamma_2)\gtrless R^{(2)}$$

- **3rd transmission attempt**

$$\frac{3/4}{3} \cdot C(5\gamma_1 + 4\gamma_2 + 4\gamma_3) + \frac{-\eta - 39/4}{3} \cdot C(5\gamma_1 + 5\gamma_2 + 4\gamma_3) +$$
$$+ \frac{\eta + 21/2}{3} \cdot C(4\gamma_1 + 5\gamma_2 + 4\gamma_3) + \frac{-\eta - 39/4}{3} \cdot C(4\gamma_1 + 5\gamma_2 + 5\gamma_3) +$$
$$+ \frac{3/4}{3} \cdot C(4\gamma_1 + 4\gamma_2 + 5\gamma_3) + \frac{\eta + 21/2}{3} \cdot C(4\gamma_1 + 4\gamma_2 + 4\gamma_3) \gtrless R^{(3)}$$

- **4th transmission attempt**

$$\frac{-\eta - 39/4}{3} \cdot C(5\gamma_1 + 4\gamma_2 + 4\gamma_3 + 5\gamma_4) + \frac{21/2 + \eta}{3} \cdot C(5\gamma_1 + 4\gamma_2 + 4\gamma_3 + 4\gamma_4) +$$
$$+ \frac{-\eta - 39/4}{3} \cdot C(5\gamma_1 + 5\gamma_2 + 4\gamma_3 + 4\gamma_4) + \frac{21/2 + \eta}{3} \cdot C(4\gamma_1 + 5\gamma_2 + 4\gamma_3 + 4\gamma_4) +$$
$$+ \frac{-\eta - 39/4}{3} \cdot C(4\gamma_1 + 5\gamma_2 + 5\gamma_3 + 4\gamma_4) + \frac{21/2 + \eta}{3} \cdot C(4\gamma_1 + 4\gamma_2 + 5\gamma_3 + 4\gamma_4) +$$
$$+ \frac{-\eta - 39/4}{3} \cdot C(4\gamma_1 + 4\gamma_2 + 5\gamma_3 + 5\gamma_4) + \frac{21/2 + \eta}{3} \cdot C(4\gamma_1 + 4\gamma_2 + 4\gamma_3 + 5\gamma_4) \gtrless R^{(4)}$$

C MARKOV CHAIN GRAPH

In this Appendix you can find in Figure 27 the graph of the proposed Markov model described in Chapter 3 on page 19.

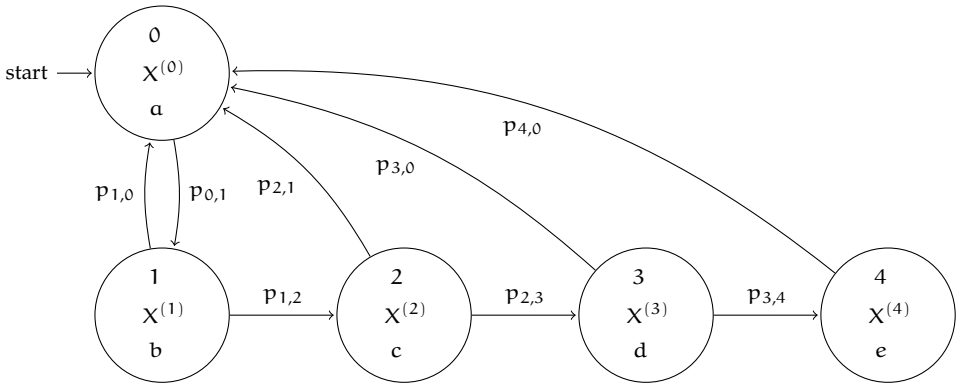

Figure 27: Graphical representation of the proposed Markov model.

The graphical representation in Figure 27 is general and, at the same time, compact: illustrating the entire Markov chain would be unfeasible, indeed. We recall that every state consists of the triplet

$$(K_n, X_n, CQI_n)$$

where

- $K_n \in \{0, 1, 2, 3, 4\}$ is the number of attempts done by the transmitter to deliver the current packet; if $K_n = 0$ it means that a new packet has just started its transmission round
- X_n is the value of the ACMI at the n-th transmission attempt; if $K_n = 0$ then it follows that $X_n = 0$
- CQI_n is the CQI index experienced during the n-th transmission attempt; if $K_n = 0$ then CQI_n is just the CQI value of the previous packet last transmission attempt, i.e., $CQI_n \equiv CQI_{n-1}$; this CQI value is used to select the appropriate MCS for the next packet transmission.

In the graph we denote with $X^{(i)}$ the ACMI relative to the transmission attempt $X_n = i$, $i \in \{0, 1, 2, 3, 4\}$. The random process starts from the state

$(0, X^{(0)}, a)$, where $a = \arg\max_i \{\pi_i\}$, and travels a random path, according to the following transition probabilities:

$$
\begin{aligned}
p_{0,1} &= \mathbb{P}[CQI_n = b \mid CQI_{n-1} = a] \\
p_{1,2} &= \mathbb{P}[X^{(1)} \leqslant R_c^{(0)} \cdot \log_2 M \, , CQI_{n+1} = c \mid CQI_n = b] \\
p_{2,3} &= \mathbb{P}[X^{(2)} \leqslant R_c^{(1)} \cdot \log_2 M \, , CQI_{n+2} = d \mid CQI_{n+1} = c, CQI_n = b] \\
p_{3,4} &= \mathbb{P}[X^{(3)} \leqslant R_c^{(2)} \cdot \log_2 M \, , CQI_{n+3} = e \mid CQI_{n+2} = d, CQI_{n+1} = c, CQI_n = b] \\
p_{1,0} &= \mathbb{P}[X^{(1)} > R_c^{(0)} \cdot \log_2 M \mid CQI_n = b] \\
p_{2,0} &= \mathbb{P}[X^{(2)} > R_c^{(1)} \cdot \log_2 M \mid CQI_{n+1} = c, CQI_n = b] \\
p_{3,0} &= \mathbb{P}[X^{(3)} > R_c^{(2)} \cdot \log_2 M \mid CQI_{n+2} = d, CQI_{n+1} = c, CQI_n = b] \\
p_{4,0} &= 1
\end{aligned}
$$

where the cardinality of the symbol alphabet M and the coding rate $R_c^{(i-1)}$ depend on the value of the CQI in the state $(0, 0, a)$, i.e.,

$$M = M(a) \text{ and } R_c = R_c(a)$$

The random rewards that we consider are

$$
\begin{aligned}
\mathcal{R}_{1,0} &= R_c^{(0)} \cdot \log_2 M \\
\mathcal{R}_{2,0} &= R_c^{(1)} \cdot \log_2 M \\
\mathcal{R}_{3,0} &= R_c^{(2)} \cdot \log_2 M \\
\mathcal{R}_{4,0} &= \begin{cases} 0 & \text{if } X^{(4)} \leqslant R_c^{(3)} \cdot \log_2 M \\ R_c^{(3)} \cdot \log_2 M & \text{otherwise} \end{cases} \\
\mathcal{T}_{1,0} &= \tau \\
\mathcal{T}_{2,0} &= 2\tau \\
\mathcal{T}_{3,0} &= 3\tau \\
\mathcal{T}_{4,0} &= 4\tau
\end{aligned}
$$

where $\tau = 8 \cdot \text{TTI}$ and, again, $M = M(a)$.

Note that this representation is general because all quantities, e.g. the CQI values, are considered as parameters.

BIBLIOGRAPHY

Blumenstein, J., J. C. Ikuno, J. Prokopec, and M. Rupp

2011 "Simulating the Long Term Evolution Uplink Physical Layer" (Sept. 2011). (Cited on p. 32.)

Bringhurst, R.

1992 *The Elements of Typographic Style*, Hartley & Marks. (Cited on p. ii.)

Caire, G., G. Taricco, and G. Biglieri

1997 "Bit-Interleaved Coded Modulation".

Caire, G. and D. Tuninetti

2001 "The Throughput of Hybrid-ARQ Protocols for the Gaussian Collision Channel", *IEEE Transactions on Information Theory*, 47, 5 (July 2001), p. 18. (Cited on p. 16.)

Cheng, J. F.

2003 "On the Coding Gain of Incremental Redundancy Over Chase Combining", *Global Telecommunications Conference (GLOBECOM)*, 1 (Dec. 2003).

2006 "Coding Performance of Hybrid ARQ Schemes", *IEEE Transactions on Communications*, 54, 6 (June 2006).

2008 "Analysis of Circular Buffer Rate Matching for LTE Turbo Code" (Sept. 2008). (Cited on p. 25.)

Dahlman, E., S. Parkvall, and J. Sköld

2011 *4G LTE/LTE-Advanced for Mobile Broadband*, Elsevier.

Ikuno, J. C., C. Mehlführer, and M. Rupp

2011 "A Novel Link Error Prediction Model for OFDM Systems with HARQ". (Cited on p. 13.)

Knuth, D. E.

1973 *Computer Programming as an Art*, vol. 3, Addison-Wesley, Reading (Massachusetts).

Kwan, R. and J. C. Ikuno

2013 "Effective HARQ code rate modelling for LTE", *Electronics letters*, 49, 7 (Mar. 2013). (Cited on p. 11.)

Makki, B.

2013 *Data Transmission in the Presence of Limited Channel State Information Feedback*, PhD thesis, Chalmers University of Technology.

Melführer, C., M. Wrulich, and J. C. Ikuno

2009 "Simulating the Long Term Evolution Physical Layer" (Aug. 2009).

Østerbø, O.

2011 "Scheduling and Capacity Estimation in LTE", *Advances in Electronics and Telecommunications*, 2, 3 (Sept. 2011). (Cited on p. 21.)

Pantieri, L. and T. Gordini

2011 *L'arte di scrivere con LaTeX*, http://www.lorenzopantieri.net/LaTeX_files/ArteLaTeX.pdf.

Quer, G., R. Rao, and M. Zorzi

2010 "Cognitive Network Inference through Bayesian Network Analysis" (Dec. 2010).

Szczecinski, L., C. Correa, and C. Ahumada

2010 "Variable-Rate Transmission for Incremental Redundancy Hybrid ARQ" (Dec. 2010). (Cited on p. 16.)

Tajan, R.

2013 *Mécanismes de retransmission Hybrid-ARQ en radio-cognitive*, PhD thesis, Université de Cergy-Pontoise.

Tuninetti, D.

2007 "Transmitter channel state information and repetition protocols in block fading channels" (Sept. 2007).